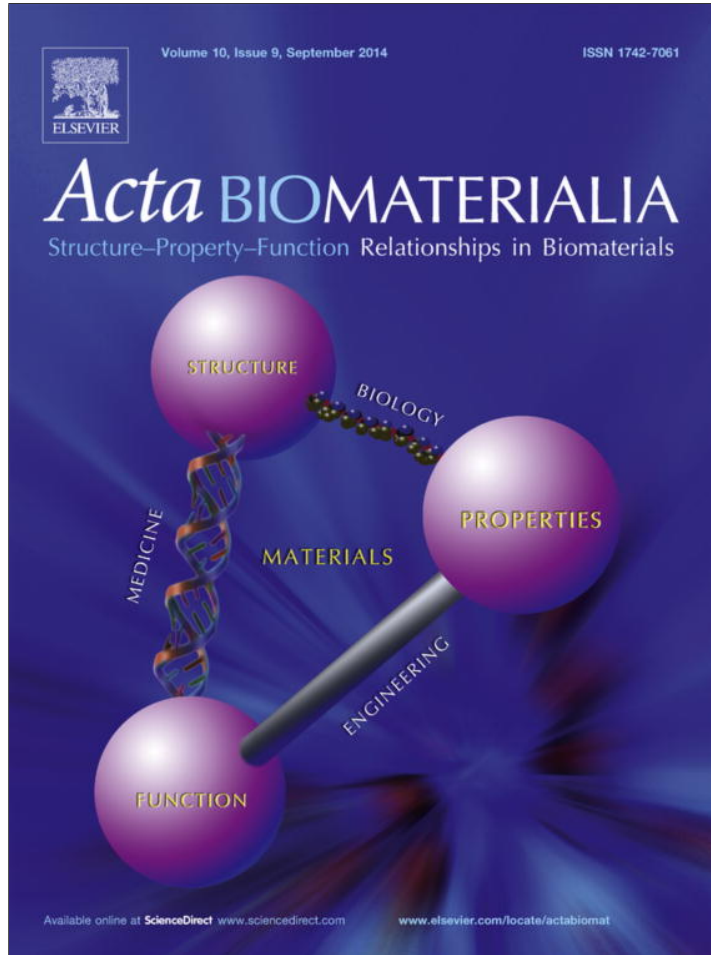


Provided for non-commercial research and education use.
Not for reproduction, distribution or commercial use.



This article appeared in a journal published by Elsevier. The attached copy is furnished to the author for internal non-commercial research and education use, including for instruction at the authors institution and sharing with colleagues.

Other uses, including reproduction and distribution, or selling or licensing copies, or posting to personal, institutional or third party websites are prohibited.

In most cases authors are permitted to post their version of the article (e.g. in Word or Tex form) to their personal website or institutional repository. Authors requiring further information regarding Elsevier's archiving and manuscript policies are encouraged to visit:

<http://www.elsevier.com/authorsrights>



Contents lists available at ScienceDirect



Review

Eggshell membrane biomaterial as a platform for applications in materials science[☆]

Matej Baláž *

Institute of Geotechnics, Slovak Academy of Sciences, Watsonova 45, 04001 Košice, Slovakia

ARTICLE INFO

Article history:

Available online 27 March 2014

Keywords:

Eggshell membrane
Application
Review
Biomaterial

ABSTRACT

Eggshell membrane (ESM) is a unique biomaterial, which is generally considered as waste. However, it has extraordinary properties which can be utilized in various fields and its potential applications are therefore now being widely studied. The first part of this review focuses on the chemical composition and morphology of ESM. The main areas of ESM application are discussed in the second part. These applications include its utilization as a biotemplate for the synthesis of nanoparticles; as a sorbent of heavy metals, organics, dyes, sulfonates and fluorides; as the main component of biosensors; in medicine; and various other applications. For each area of interest, a detailed literature survey is given.

© 2014 Acta Materialia Inc. Published by Elsevier Ltd. All rights reserved.

1. Introduction

The eggshell membrane (ESM) is a part of an egg that contains certain essential and widely used nutrients. The utility of ESM, together with eggshell (ES), has long been underestimated because it was considered waste material. However, it is today being widely studied because of its unique properties, which are a result of its fascinating structure. This review focuses on recent applications of ESM. The research community has made significant progress in studying this exceptional biomaterial, and a wide variety of applications have been discovered. In 2011–2013, the number of published papers on ESM was >30 per year, proof that this material is of significant interest in various areas of science (Fig. 1).

Recent review papers dealing with this topic include the ones published by King'ori in 2011 [1], and by Guru and Dash in 2014 [2]. However, both of these papers concentrate on eggshell waste as a whole (both ES and ESM are discussed). No review dealing so-

lely and in detail with the applications of ESM has yet been published.

Historically, the very first paper dealing with ESM was published by Robinson and King [3] in 1963 (not included in Fig. 1). This paper discussed the role of ESM in the process of the ES formation. At that time, scientists paid little attention to the role of ESM in this process because it was generally believed that ES formation was influenced mainly by the enzyme carbonic anhydrase.

Among the oldest papers dealing with ESM is the one by Osuji et al. from 1971 [4]. This dealt with the acid glycosaminoglycan content in the ESM, and also compared this with its content in the isthmus region of the hen oviduct (where ESM is secreted). The potential role of hyaluronic acid in water retention and resistance to bacterial attack was also proposed in this work.

From that time onwards, a large number of works have published on depicting the structure of ESM. Many of these will be mentioned in the corresponding parts of this review.

Because this review is devoted to the applications of ESM, the paper by Wu et al. published in 1995 should definitely be mentioned [5]; this can be considered as the first paper to discuss real applications of ESM and not only its structural characteristics. *In vitro* demineralized ESM was used to investigate the *in vitro* modulation of calcite CaCO_3 crystal deposition. ESM was shown to be a good platform for the crystallization. Today, a very wide spectrum of applications of ESM is available.

1.1. Separation from the eggshell

If ESM is to be utilized, it has to be separated from the ES after processing of the eggs. As will be described in next part of this

Abbreviations: ESM, SM, eggshell membrane; ES, eggshell; LM, limiting membrane; DAF, dissolved air flotation; ML, mammillary layer; PL, palisade layer; MB, mammillary bodies; OSM, outer eggshell membrane; ISM, inner eggshell membrane; SMF, shell membrane fibers; SEP, soluble eggshell membrane protein; JCT, joint and connective tissue; PEMFCs, proton exchange membrane fuel cells; NPs, nanoparticles; SOFCs, solid oxide fuel cells; ASP, alternating soaking process; SERS, surface enhanced Raman scattering; LDH, layered double hydroxide; SPE, solid phase extraction; FAAS, flame atomic absorption spectrometry; HG-AFS, hydride generation atomic fluorescence spectrometry; LAS, linear alkyl benzene sulfonates; GO_x , glucose oxidase; CL, chemiluminescence; GTR, guided tissue regeneration.

* Part of the Biominerization Special Issue, organized by Professor Hermann Ehrlich.

* Tel.: +421 557922603; fax: +421 557922604.

E-mail address: balazm@saske.sk

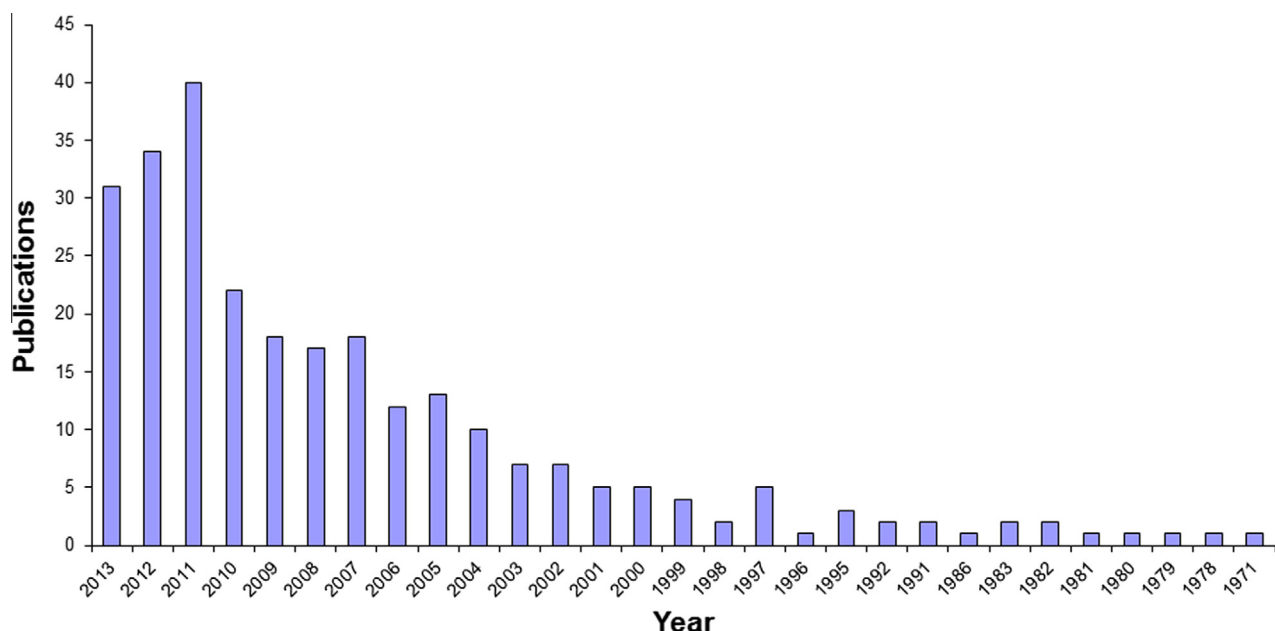


Fig. 1. Number of papers dealing with eggshell membrane published in the years 1971–2013.

paper, ESM is composed of three layers: (i) outer ESM, (ii) inner ESM and (iii) limiting membrane (LM). The inner ESM and LM can be separated mechanically; however, the outer ESM is strongly embedded into the ES and in general acidic treatment (e.g. dilute acetic acid, HCl or EDTA) is required to separate it from the ES [6–16]. The separation in acidic conditions can be performed in two ways: (i) by dissolving calcite (CaCO_3), which is the main component of the ES, in acid, [6–9]; or (ii) by immersing the ES in acid (which does not completely dissolve the ES but allow the ESM to be separated from the ES) [10–14]. Despite the strong embedding of the outer ESM in the ES, in some works [17–21] simply stripping the outer ESM from the ES was reported as being sufficient.

Another recently developed method for ES–ESM separation is dissolved air flotation (DAF) [22]. Using a DAF separation unit, it is possible to recover 96% of ESM and 99% of calcium carbonate present in the ES from ES waste within 2 h of operation.

The separation of ESM from ES will be a key process if ESM is going to be widely applied on an industrial scale. Therefore considerable attention should be devoted to this particular step.

2. Properties

2.1. Structure and morphology

ESM is a fibrous structure situated between the ES and the egg white. It is a biopolymeric fibrous net, which is essential for the formation of ES and which provides a non-mineralized platform for the outer mineralization of ES, while, on the other hand, preventing the mineralization of egg white from the inside [23,24]. Fig. 2 illustrates the structure of ESM. An artistic rendition of the cross-sectional view of an ES is given in Fig. 2a, where in the lower part both the inner and outer ESM can be seen. The localization of the ESM in the whole egg is shown in Fig. 2b. The upper inset shows a schematic view describing all the substructures of the ESM, and the lower inset is a photograph of the inner ESM.

As noted above, and as can be seen from the upper inset in Fig. 2b, the ESM can be divided into three parts: the outer ESM, the inner ESM and the LM. These three structures have different morphologies.

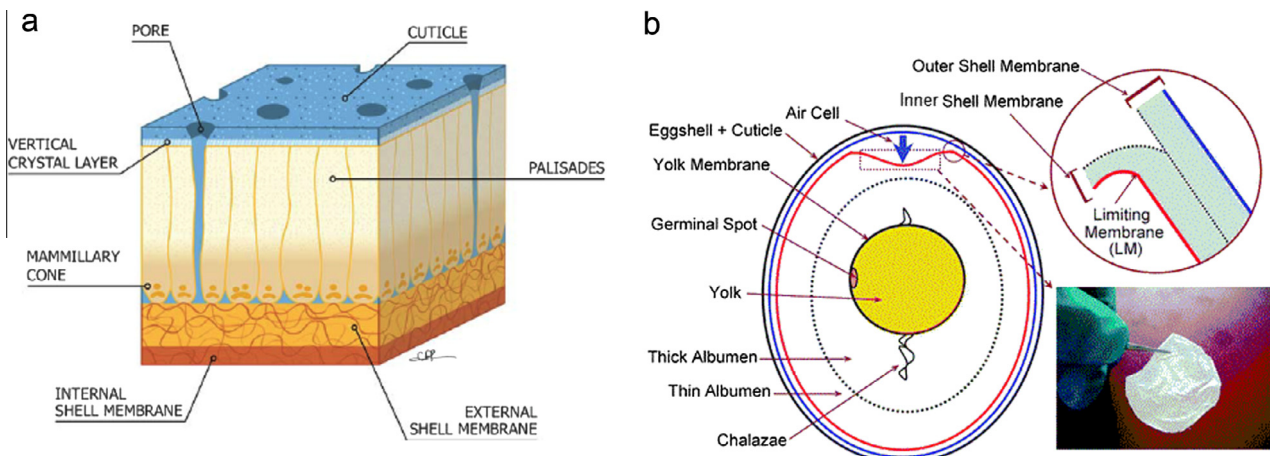


Fig. 2. (a) Artistic rendition of a cross-sectional view of eggshell [25]; (b) structure of egg (upper inset: substructures of the ESM; lower inset: photograph of the inner ESM). Modified from Ref. [26].

The outer ESM is located just under the ES and its fibers range in thickness between 1 and 7 µm. The fibers of the outer shell membrane extend into the mammillary knobs of the shell. The thickness of the whole outer membrane layer is ~50–70 µm [27,28].

The inner ESM is separated from the outer ESM by the space filled with air, which is the biggest in the air cell (Fig. 2b). In comparison with the outer one, the fibers of the inner membrane are smaller in diameter [27]—their thickness ranges from 0.1 to 3 µm—and in addition the whole inner membrane layer is thinner—its thickness is between 15 and 26 µm. The fibers of the inner ESM are interlaced with the outer membrane [28].

The LM represents the innermost very thin structure of the ESM which surrounds the egg white [29]. Liong et al. reported that after staining with fluorescein isothiocyanate (FITC), the LM appears as particles that fill the spaces between the inner membrane fibers several microns outward from the level at which the inner membrane fibers first appear [28].

Scanning electron microscopy (SEM) images showing the positioning of the ESM within the ES and the morphology of its substructures are shown in Fig. 3.

In general, the shell membrane fibers are arranged in layers parallel to the surface of the egg [27]. These layers are discernible because of changes in fiber position, orientation and size [28]. No relationship between the positioning of the mammillary knobs and the patterning of the shell membrane was discovered; however, it is suggested that the positioning of the knobs reflects the pattern of certain secretory cells in the genital tract of the hen [27].

The individual fibers are randomly orientated and may extend for distances of at least 25 µm [27], and, according to Torres et al., seem to be formed by several fibrils [18]. A fibril 102 nm high and 370 nm wide was observed. The fibrils are composed of a core with a high electron density and outer, less-electron-dense mantle. They are separated by extrafiber spaces [19]. SEM and TEM images of the fibers of the outer ESM are shown in Fig. 4a and b, respectively.

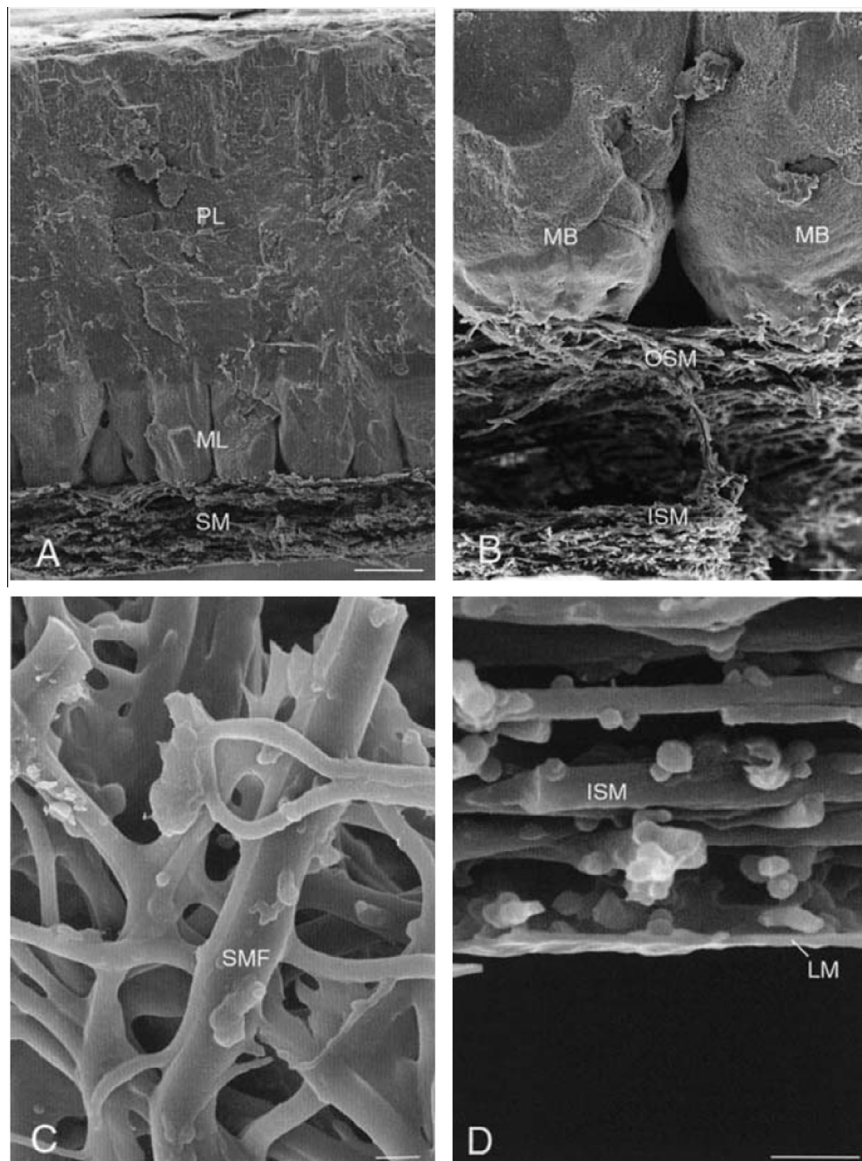


Fig. 3. Scanning electron micrographs illustrating the morphology of the eggshell and eggshell membranes: (A) eggshell cross-fractured to reveal different layers of the eggshell (mammillary layer, ML and palisade layer, PL and the eggshell membrane, SM); (B) higher magnification of the ESM-mammillary body interface (mammillary bodies, MB, outer ESM, OSM, inner ESM, ISM); (C) enlargement of the shell membrane fibres, SMF to reveal their interwoven and coalescing nature; (D) inner aspect of the inner ESM, ISM, demonstrating the limiting membrane, LM that surrounds the egg white. Scale bars: A = 50 µm; B = 20 µm; C and D = 2 µm. Reprinted with permission from Ref. [30].

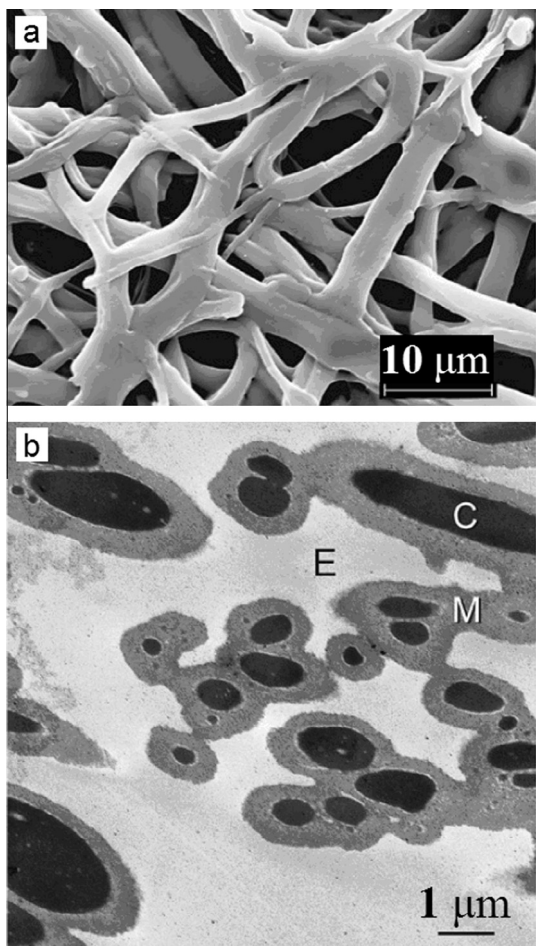
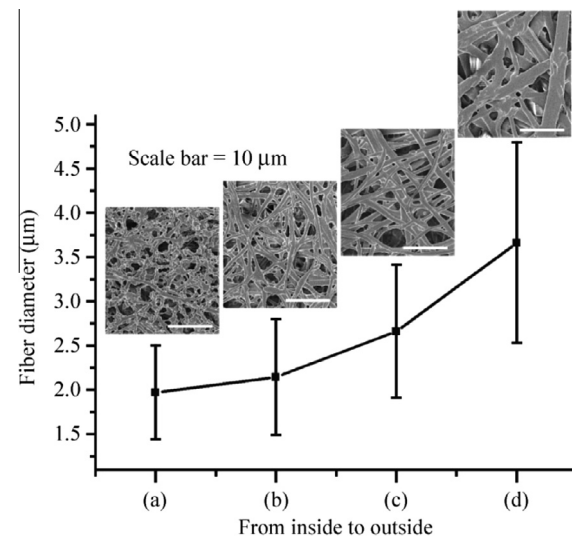


Fig. 4. SEM (a) and stained TEM (b) image of the outer ESM. C, core; M, mantle; E, extrafiber spaces. Reprinted with permission from Ref. [19].

Zhou et al. have performed an extensive study on the morphology of both ESM and ES [7]. Their observations of the ESM are shown in Fig. 5. Comparing the outer and inner surfaces of the



© Copyright 2011, Springer.

Fig. 6. Diameter of the fiber membrane from the inside to the outside: (a) inner surface of the inner membrane; (b) outer surface of the inner membrane; (c) inner surface of the outer membrane; (d) outer surface of the outer membrane. Reprinted with permission from Ref. [7].

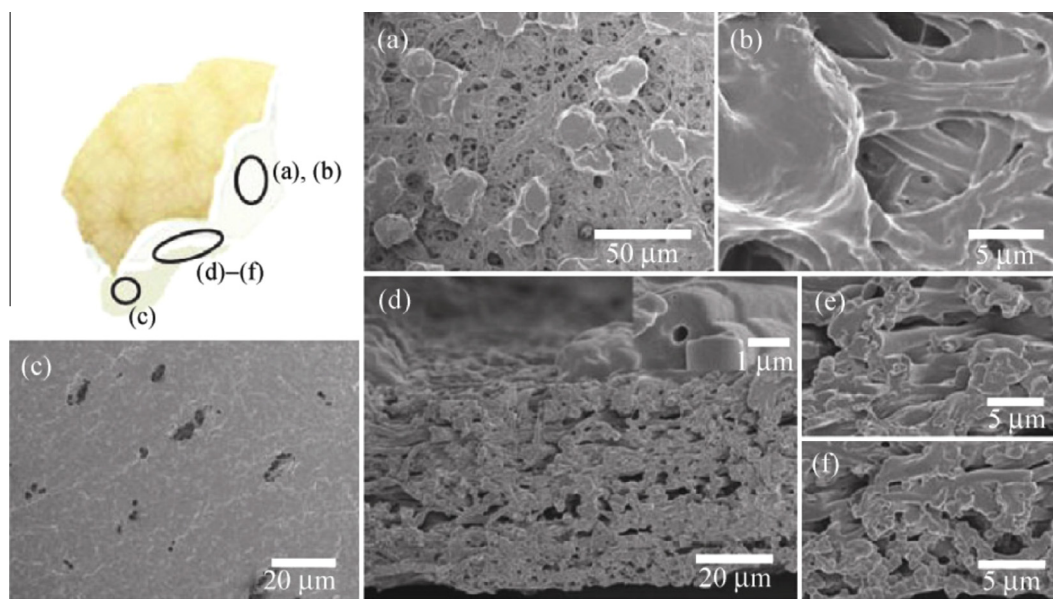
ESM, there are knobs formed by the assembly of more fibers present on the outer surface. The inner surface of the ESM is much smoother, and in general the inner membrane is a more compact structure than the outer [7].

The diameter of the fibers was also studied in detail in Ref. [7]. The decrease in the diameter of the fibers from the outer side to the inner side of the ESM was confirmed (Fig. 6) and fiber sizes of 2.5–5 μm at the surface of the outer ESM and 1.5–2 μm on the inner side of the inner ESM were observed.

The morphology of the ESM strongly influences its properties. The mechanical properties of the ESM were extensively studied by Torres et al. [18].

2.2. Chemical composition

Many authors have investigated the constituents of the ESM [31–34]. The fibers of ESM are composed mainly of proteins



© Copyright 2011, Springer.

Fig. 5. SEM images of the eggshell membrane: (a,b) outer surface with many knobs; (c) smooth inside face (contacting the egg white); (d) cross-section—the inset is the section of a single fiber, exhibiting a core–cortex structure with holes inside; (e) magnified image of the outer ESM; (f) magnified image of the inner ESM. Reprinted with permission from Ref. [7].

(80–85%), of which ~10% are collagens (types I, V and X) and 70–75% are other proteins and glycoproteins containing lysine-derived cross-links [33,35–39]. The number of proteins present in the whole ES matrix (ES + ESM) is >500, which is almost 4–5 times higher than those found in other egg compartments (i.e. 148 proteins in the egg white, 137 in the vitelline membrane and 316 in the egg yolk) [40–45]. Recently, the presence of 62 proteins solely in the ESM was reported [34].

In the work by Wong et al. [38], the ratio between collagens I and V was estimated to be 100:1. The presence of collagen in ESM was confirmed by immunochemical tests [38,46,47]. Providing the complete protein composition of ESM is beyond the scope of this review article; however, some proteins typical for this particular structure can be highlighted: e.g. lysozyme [30], ovotransferrin [48], ovalbumin [49], ovocalyxin-36 [50,51], desmozime and isodesmoxime [24,52]. Other proteins that are present in ESM are osteopontin, sialoprotein and keratin [53]. The detailed protein composition of the whole ES matrix can be found in literature (e.g. [24,25,29,53,54]).

Each fiber consists of a collagen-rich core and a glycoprotein-rich cortex [24,55]. It was shown recently that the amount of collagen, which is important for various applications (e.g. medical burn treatment or manufacturing of cosmetics), can be increased by adjusting the diet of the hen [56].

The outer and inner ESM differ slightly not only in morphology, but also in their chemical composition. The cores of the fibers of the outer ESM contain mainly type I collagen and the inner ESM core proteins contain mainly types I and V collagen [57]. Collagen X was identified in both membranes [46] and is believed to facilitate the inhibition of mineralization of the ESM [23]; however, its localization in the core of the fibers [46] does not support this hypothesis [24]. The inner ESM is not calcified, but the fibers of the outer ESM are partially mineralized and incorporated into the mammillary layer of the eggshell [23,24]. According to Bellairs and Boyde [27], there is no keratin present in the cortex of the fibers. The LM is also formed from this cortex.

Nakano et al. have reported an extensive study on the amino acid composition of both inner and outer ESM [58] (see Table 1).

Proline, glutamic acid and glycine are the most abundant in ESM with contents >10% in both membranes. However, Nakano et al. did not report the presence of cysteine and hydroxylysine [58]. On the other hand, Li et al. measured their content as 5.27% and 0.19%, respectively [19]. Kodali et al. [59] reported a cysteine content of ~10% and claimed that this relatively high content of cysteine may be a result of the presence of a considerable amount

of cysteine-rich eggshell membrane proteins (CREMPs) with multiple disulfide crosslinks. It is possible to determine the exact locations of cysteine in ESM [60]. Hydroxylysine suggests the presence of collagens in the structure of ESM [19]. This is supported by the fact that ESM is digested by the enzyme collagenase [24].

ESM contains also non-protein entities, from which the presence of sialic and uronic acid can be highlighted [58]. In addition, a small amount of saccharides is present [53].

Because of the practical insolubility of ESM, which is a result of the large number of disulfide bond crosslinks [61], and because the shape and size of the ESM are not easily controllable, applications of ESM are limited. However, it is possible to overcome these problems by preparing an ESM protein that is soluble in common non-toxic solvents but insoluble in water. Such material is referred to as soluble eggshell membrane protein (SEP) [62,63]. By utilization of 3-mercaptopropionic acid, acetic acid, heating and centrifugation, it is possible to isolate SEP from ESM [62].

2.3. Further characterization of ESM

Many authors have investigated ESM by the means of infrared spectroscopy. A characteristic Fourier transform infrared spectrum of ESM is shown in Fig. 7.

The infrared spectrum of ESM can be divided into two regions: the first one between 3750 and 2500 cm⁻¹, and the other one below 1700 cm⁻¹. In the region with higher wavelengths, the most intensive peak is evidenced at 3287 cm⁻¹, which corresponds to the stretching mode of O–H and N–H groups. Peaks at 3060, 2932 and 2869 cm⁻¹ correspond to the asymmetric stretching vibrations of the C–H bonds present in =C–H and =CH₂ groups [65,66]. In the region with lower wavelengths, the peaks at 1630 cm⁻¹ (C=O), 1530 cm⁻¹ (CN stretching/NH bending modes) and 1234 cm⁻¹ (CN stretching/NH bending modes) can be assigned to the amide I, amide II and amide III vibrations of the glycoprotein mantle of the fibers, respectively [67–70]. The peaks at 1448, 1073 and 620 cm⁻¹ correspond to the stretching modes of C=C, C–O and C–S bonds, respectively [39,67,71–75].

The thermal stability of ESM is naturally not very high, because it contains proteinaceous fibers. The thermogravimetric curve of ESM is given in Fig. 8, from which it can be seen that thermal decomposition of ESM is a multistep process starting very early (around 55 °C). At this temperature, the thermal denaturation of collagen takes place [76]. The first stage of decomposition is finished around 120 °C. The second stage of decomposition, which might be a consequence of the thermal degradation of collagen [76], takes place in the range between 250 and 450 °C. In case of

Table 1
Amino acid content in inner and outer ESM in mol.%. Modified with permission from Ref. [58]. Copyright 2003, Poultry Science Association.

Amino acid	Inner ESM	Outer ESM
Proline	11.6	12.0
Glutamic acid	11.1	11.9
Glycine	11.1	10.6
Serine	9.2	9.2
Hydroxyproline	1.5	1.4
Aspartic acid	8.4	8.8
Valine	7.2	7.9
Threonine	6.9	6.9
Arginine	5.7	5.8
Leucine	5.6	4.8
Alanine	4.6	4.1
Histidine	4.1	4.3
Lysine	3.6	3.4
Isoleucine	3.3	3.4
Methionine	2.3	2.3
Tyrosine	2.2	1.7
Phenylalanine	1.6	1.5

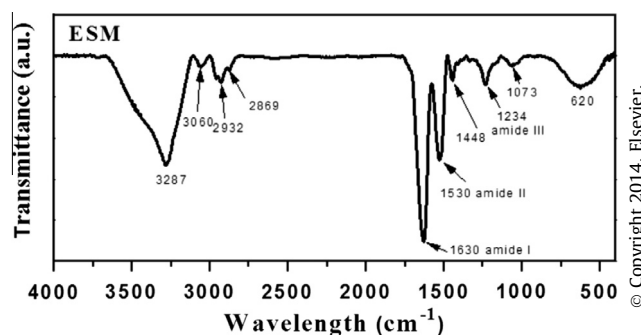


Fig. 7. Infrared spectrum of ESM. Modified with permission from Ref. [64].

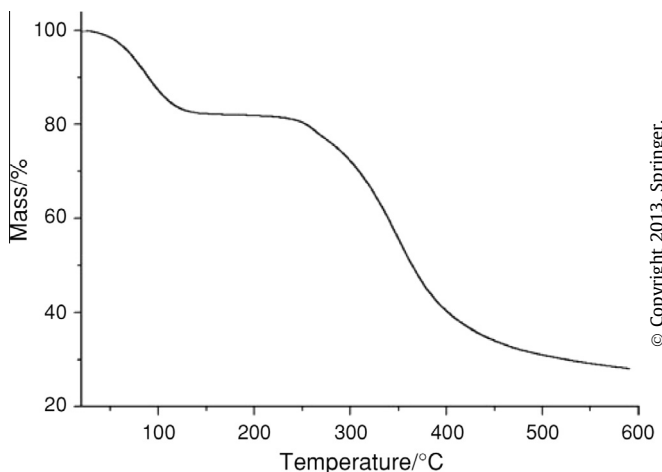


Fig. 8. Thermogravimetric curve of the eggshell membrane. Reprinted with permission from Ref. [76].

higher temperatures, the slow continuous decrease of mass loss continues.

The mechanical properties of ESM were investigated in depth by Torres et al. [18]. In some respects, the mechanical behavior of ESM is similar to other biopolymer materials (e.g. tendons, collagen and DNA molecules). In all these systems, nonlinear elasticity was evidenced, as a consequence of the entropic and enthalpic contributions of the molecules present in their structures. The entropic mechanisms of the deformation of the collagen molecules present in ESM are the main driving force at low strain levels. When a higher level of strain is applied, the mechanical behavior of ESM is similar to that of other fiber networks and cellular solids. The fact that the environmental conditions influence the mechanical properties of ESM was confirmed by the axial tests. If ESM was subjected to water, the interaction of water with the biopolymer molecules was observed, and hence it can be concluded that water acts as a plasticizing agent in this case [18]. Later, the same group carried out a study dealing with the effect of the temperature on the mechanical properties of ESM [76]. The results of the uniaxial tensile tests showed that the Young's modulus of ESM decreases with increasing temperature. By means of differential scanning calorimetry, it was shown that the more water is present in the material, the higher is the peak temperature of denaturation of the proteins. The authors explained this fact by the ability of water molecules to form hydrogen bonds with amide groups of the ESM [76]. A detailed study dealing with the resistance to mechanical penetration of ES and ESM was reported in Ref. [77]. The most important facts presented there are: (i) the outer ESM acts as a strong adhesive agent between the inner ESM and the eggshell; (ii) the penetration energy required from outside the ES (containing ESM) is larger than that from the inside because it includes the energy required to break the ESM and peel it off the ES.

2.4. Modification of ESM

Although ESM with its unique structure can be utilized in wide variety of fields, its application in natural form is not suitable for certain applications. To overcome this problem, its composition and morphology can be modified by several procedures (e.g. thiolation [78,79], modification of the pore size and fiber crossing density [72] or transformation to SEP [62,63]). Another way of modifying ESM involves its mineralization. Li et al. [19] utilized ESM as a universal model for differential biomimetic calcification and silicification. The properties of ESM were manipulated to render it permeable to stabilized mineral precursors and the possibil-

ity of introducing nanostructured calcium phosphate or silica into ESM fiber cores or mantles was confirmed. The potential of the ESM to be mineralized by different mineral species at different locations was also noted [19].

3. Applications

The unique properties of ESM are clearly interesting for various fields of application. Research activity has concentrated mainly on three fields: (i) the utilization of ESM as a biotemplate for the synthesis of various nanoparticles; (ii) the potential of ESM as a sorbent of various species, including heavy metal ions and organic dyes; and (iii) the application of ESM as a biosensor. However, ESM also represents an interesting biomaterial for other fields, such as medicine (e.g. ESM as a therapeutic for joint and connective tissue (JCT) disorder) or electrochemistry (e.g. ESM as a separator in supercapacitors).

3.1. ESM as a biotemplate

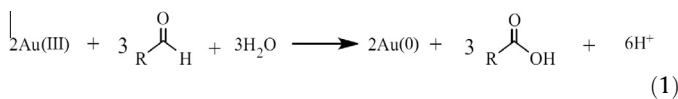
The entangled structure of ESM fibers has inspired many scientists, who have used them as a platform for the growth of nanocrystals. Chemical entities with various structures and compositions, ranging from pure nanocrystalline elements to complicated non-stoichiometric compounds, were successfully prepared by utilizing ESM as a template. The compounds are produced in the form of composite with ESM. In order to remove the ESM and achieve better crystallization of the inorganic sinters, these composites are then calcined at temperatures of up to 600 °C.

Elemental nanocrystalline gold and iron were prepared in Ref. [80]. The authors prepared nanoclusters bound on ESM. These materials can be utilized as recyclable catalysts and materials suitable for fluorescence and Raman spectroscopy methods. Nanoparticles of sulfur with sizes of 5–35 nm were prepared with ESM and Tween-80 surfactant by Cheng et al. [81]. Flexible platinum and silver catalysts with a network structure doped with polyaniline and polypyrrole were synthesized by Tang et al. [82]. The catalytic activity of these materials was studied for the methanol oxidation reaction, in which they should serve as proton exchange membrane fuel cells (PEMFCs). The morphology of the metal components was different depending on the polymer used. Cyclic voltammetry studies at ambient temperature have shown excellent photocatalytic activity of these catalysts for reaction in an acidic environment. The potential of these materials to be used as high-temperature PEMFCs was also studied, and because their activity increases at higher temperatures, they appear suitable for this application [82]. In Ref. [83] the activity of a catalyst based on silver nanoparticles (AgNPs) bound on the ESM for the same reaction was studied. The results were also positive from the point of view of both ambient- and high-temperature PEMFCs.

ESM exhibits a particular ability to reduce metals from their solutions into the elemental state. Ashraf et al. produced nanoparticles of gold on ESM without using additional reducing agents [84]. These authors also studied the effect of pH. Lower pH favored the formation of irregularly shaped but dense gold macro/nanocrystals, whereas higher pH (8–9) favored the formation of fairly uniform but less dense gold nanoparticles (AuNPs). In addition, Ashraf et al. have studied the effect of heating on the templating ability of ESM. In that case, the composites of AuNPs were formed at pH 8–9, which led to the formation of highly porous, membrane-like gold while mimicking the original structure of the ESM. The potential applications of this material lie in catalysis, biosensors, electrode materials, optically selective coatings, heat dissipation and biofiltration [84].

Devi et al. [6] used ESM for the synthesis of AuNPs from a solution of Au(III) ions. They managed to obtain a stable colloidal suspension of AuNPs with particle sizes <20 nm. In addition, they proved the potential of ESM to uptake precious metals from wastewater from their observation that AuNPs bind to the surface of ESM. The authors observed the color changes after the immersion of ESM into a solution of chloroauric acid (HAuCl_4) of two different concentrations: 10^{-2} and 10^{-4} M. In the interval between 5 and 8 h after the immersion, the decoloration of the dark yellow solution through light yellow to transparent was observed, which marks the complete disappearance of Au(III) ions from the solution. Afterwards, the color changed to pink in the case of lower concentration and blue in the case of higher concentration of acid, respectively. The presence of pink/blue color is the proof of the successful reduction of gold ions into elemental gold. Together with the color of the solution, the color of the membrane also changed (see Fig. 9a–c).

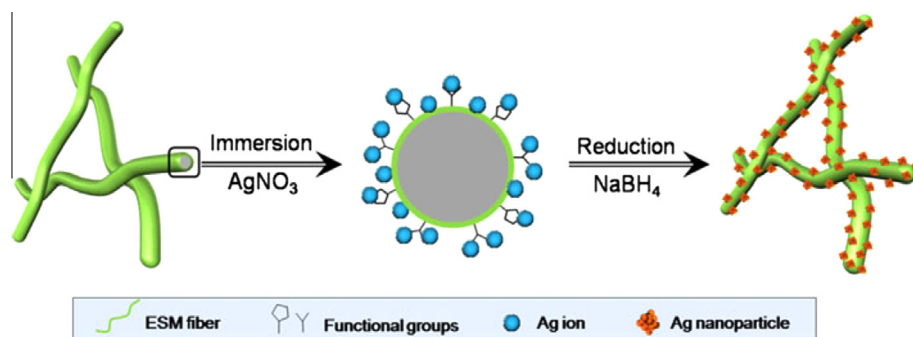
The mechanism of reduction was discussed in Ref. [85]. Because the main components of ESM are amino acids, and uronic acid is also present [58], there is a huge number of amine, hydroxyl and carbonyl groups. ESM also contains saccharides, which, together with the uronic acid, contain the aldehydic group ($\text{R}-\text{CHO}$) and they can act as reduction agents able to reduce adsorbed gold ions into elemental gold. The reduction of Au(III) by the aldehydic group can be described by the following equation:



AgNPs were deposited onto the surface of ESM in order to prepare a novel functional bio-nanocomposite [86]. The synthetic process is schematically illustrated in Fig. 10. The synthesized AgNPs were uniformly distributed and their size was in the range of 2–6 nm. The as-prepared AgNPs/ESM composite was used as a solid-phase heterogeneous catalyst for the reduction of 4-nitrophenol and exhibited a good catalytic activity.



Fig. 9. ESM photographs before (a) and after the impregnation in 10^{-4} M (b) and 10^{-2} M (c) chloroauric acid solution . Modified from Ref. [6].



© Copyright 2014, Springer.

Fig. 10. Schematic illustration of the synthesis of AgNPs deposited on ESM. Reprinted with permission from Ref. [86].

However, not only elements, but also binary compounds can be synthesized using ESM as a template. The syntheses of chalcogenides and oxides has been performed by the research group led by Su [13–15,17]. This group has synthesized nanoparticles of lead selenide (PbSe) on ESM [14]. By modifying the experimental conditions, these researchers were able to obtain nanoclusters or nanocubes of PbSe. In other words, they successfully synthesized nanocrystalline lead sulfide (PbS) [13] and cadmium sulfide (CdS) [15]. The fibers can serve also as a bioplatform for the synthesis of polyhedra of zinc oxide (ZnO) [17]. SEM images of the synthesized compounds are given in Fig. 11.

Macroporous ZnO membranes were prepared by utilizing inner ESM as a biotemplate after performing low-temperature ZnO atomic layer deposition [26]. The product exhibited strong photocatalytic effect, high mechanical flexibility and good bactericidal efficiency.

Dong et al. [87] have used ESM as a platform for the synthesis of the nanoparticles of three different oxides. For each of these, particles of different size were obtained: 5.4 nm for ZnO , 9.5 nm for Co_3O_4 and 11 nm for PdO . Nanoparticles of Mn_3O_4 were also synthesized using ESM [88]. Thermal treatment was used by Camarata et al. [89] to synthesize TiO_2 nanofibers using ESM as a biotemplate.

Recently, ESM was used for the facile synthesis of BaWO_4 nanoparticles [90]. Under optimum conditions, the synthesized nanoparticles exhibited a size of 14 nm.

ESM can also be utilized for the synthesis of ceramic materials, as was documented in Ref. [91]. A material based on the perovskite $\text{Sm}_{0.5}\text{Sr}_{0.5}\text{CoO}_3$ (SSC) was found to retain its entangled fibrous structure up to 1000 °C and can be used as a cathode in solid oxide fuel cells (SOFCs). Its properties were compared to ceramic materials obtained in a standard way and it was shown that the novel material is more suitable for this particular application [91].

1-D amorphous tris(8-hydroxyquinoline)aluminum(III) nanowires were successfully synthesized by a simple and economical

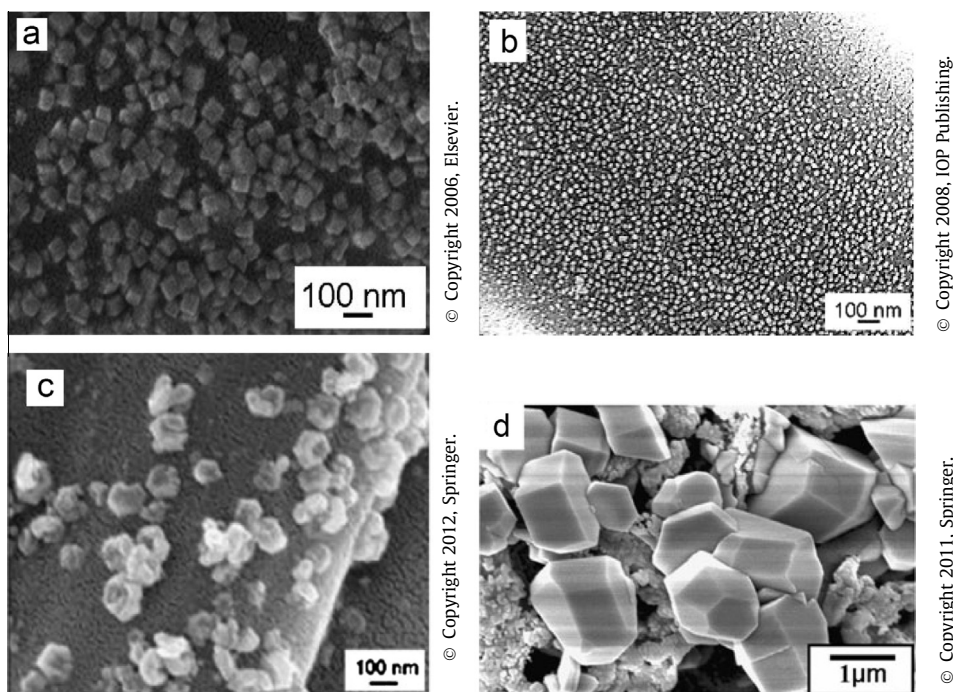


Fig. 11. SEM images of various compounds synthesized by Su et al.: (a) PbSe, (b) PbS, (c) CdS, (d) ZnO polyhedrons. Reprinted with permissions from (a) Ref. [14]; (b) Ref. [13]; (c) Ref. [15]; (d) Ref. [17].

method using ESM as a template [20]. The nanowires, 1–2 μm long and $\leq 400 \text{ nm}$ wide, exhibited large specific surface area, amorphous structure and relatively high photoluminescence intensity. The potential applications of the synthesized products include growing of hierarchical structures of other organic semiconductors, surface modifications of fibers and the evaporation of active pharmaceutical ingredients on medical textiles [20].

The biotemplating ability of ESM can also be utilized for the dry reforming of methane [92,93]. ESM was used as a template for NiO/CeO₂ catalysts which were then used for this purpose.

ESM has been used as a biotemplate for the synthesis of hierarchically ordered NiO-Ce_{0.8}Gd_{0.2}O_{1.9} (GDC) composite anode powders, which were then used as anodes in SOFCs [64].

A substrate for surface-enhanced Raman scattering (SERS) based on porous carbon film supported AuNPs was prepared using ESM as a template [94]. As a result, a good SERS signal was obtained and therefore ESM can be utilized in a facile and green approach to an ultrasensitive SERS substrate.

3.1.1. Biomineralization studies

In addition to ESM serving as a biotemplate for various compounds, a considerable amount of work dealing with the use of ESM as a substrate for studying the unique crystal calcium carbonate crystal growth processes of biomineralization has been performed [5,57,95,96]. In these works, the process of synthesis of calcium carbonate crystals is often compared to the natural biomineralization process.

In work by Wu et al. [5] the *in vitro* modulation of calcium carbonate crystal deposition on demineralized ESM was studied. The crystallization took place almost exclusively at the peripheries of residual calcium reserve assemblies, in which a high amount of sulfur is also present. CaCO₃ crystals with a typical rhombohedral morphology on the outer surface of the ESM were produced by the incubation of EDTA-treated eggshell membrane in CaCl₂ solution in the presence of (NH₄)₂CO₃. After 24 h of incubation, the lat-

eral dimensions of the produced crystals were $\sim 5\text{--}10 \mu\text{m}$. The preferred orientation of the crystals could not be determined. The distribution of *in vitro* formed crystals was similar to that of the residual calcite observed on naturally decalcified ESM. However, if crude preparations of shell matrix extract were added to the calcium chloride solution, the morphology and size of the produced crystals was significantly affected. The addition of a small amount of eggshell matrix extract resulted in a substantial decrease in the crystalline size, whereas when higher concentrations of shell matrix extract were used, the morphology was changed to such extent that no distinct crystals were observed. The kinetics of crystal growth and the crystal distribution was not affected by the addition of the eggshell matrix extract [5].

Carrino et al. [57] added various amounts of dermatan sulfate proteoglycan isolated from the pallisade matrix of the ES to the solution from which the crystals were deposited on the demineralized ESM. This resulted in a change in crystal morphology, namely the crystals were smaller and more rounded, which more closely approximated the appearance of the natural calcium carbonate crystals present in ES.

In the work by Fernandez et al. [95], the effect of dermatan sulfate and carbonic anhydrase on the *in vitro* calcification of non-mineralized ESM-mammillae substrate was pursued, with the focus on different pH and incubation times. In this work, pieces of non-calcified ES containing recently formed mammillae were obtained from eggs at 5 h 30 min post-oviposition, where no calcium had already been deposited [36]. In Fig. 12, the morphology of calcium carbonate crystals obtained at different pH is compared.

If the substrate was incubated in CaCl₂ at pH 7.4, small calcite crystals growing on each mammilla were visible. However, incubation at pH 9.0 resulted in significantly larger calcite crystals with the sizes of 10–20 μm . The preferred orientation was {104}. Based on the results of the evaluation of the roles of dermatan sulfate and carbonic anhydrase in the process, it was concluded that the former modifies the crystal morphology, producing aggregates of

large calcite crystals exhibiting a columnar morphology and contributes to the ES texture development, whereas the latter increases the velocity of crystal growth and eventually contributes to the fusion of the crystal aggregates [95].

Demineralized ESMs were used as a substrates for the deposition of CaCO_3 -gelatin composite in Ref. [96], where the automated alternating soaking process (ASP) was applied. In addition, glass cover slips were used for the same purpose. The results show that by altering the amount of gelatin in the ionic growth solutions, the final organic component of the mineral can be regulated over the range of 1–10%, similar to that of natural ES. Within this study, it was shown for the first time that it is possible to co-precipitate CaCO_3 -gelatin composite by an ASP and that the organic fraction of this mineral can be tuned to mimic that of natural biomineralized composites.

Further studies dealing with this topic have been elaborated [19,97]; however, it is beyond the scope of this review article to discuss the details of these.

3.2. ESM as a sorbent

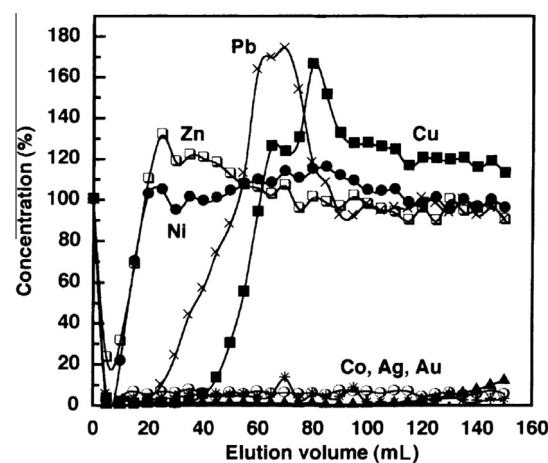
ESM can also be used as natural biosorbent: contaminated water can be cleared of various undesirable species, including heavy metal ions or organic dyes.

3.2.1. Sorption of heavy metals

Ishikawa et al. [10] have proven that ESM is able to adsorb gold from wastewater and therefore can be used for its purification. They have studied the sorption of Au(I) and Au(III) ions. From the kinetic point of view, the sorption process can be characterized by the Langmuir isotherm. Maximum sorption capacities of 147 and 618 mg g⁻¹ for Au(I) and Au(III), respectively, were achieved. The optimum pH for the sorption was 3. These authors have also demonstrated the positive effect of the miniaturization of particles on the sorption activity of ESM. Moreover, the selective sorption of various ions from electroplating wastewater was observed (Fig. 13). These authors have applied ESM as a sorbent in column chromatography using the electroplating wastewater as the eluent.

As can be seen from Fig. 13, the ability of ESM to adsorb the ions present in wastewater decreases in the following order (in parenthesis, the amount of metal ion taken up is given in percent): Au(III) (98%) > Ag(I) (97%) > Co(II) (94%) > Cu(II) (17%) > Pb(II) (15%) > Ni(II) (4%) > Zn(II) (3%). Based on these results, ions can be divided into three groups: (i) ions being almost completely taken up by the ESM (Co(II), Ag(II), Au(III)); (ii) ions being taken up hardly at all (Ni(II) and Zn(II)); and (iii) ions being partly adsorbed and after some time desorbed again (Cu(II) and Pb(II)) [10].

The sorption of Cr(VI), Cd(II) and Cu(II) ions from the model solutions by ESM was studied by Liu et al. [98]. As can be seen from



© Copyright 2002, Elsevier.

Fig. 13. Recovery of metal ions from the electroplating wastewater by ESM column, expressed as a percentage of initial metal concentration in mg l^{-1} : Co (○), 0.01; Ni (●), 0.53; Cu (■), 5.26; Zn (□), 0.56; Ag (*), 0.03; Au (▲), 23.74; Pb (x), 0.14. Reprinted with permission from Ref. [10].

Table 2

Optimum experimental conditions for the sorption of different ions [98].

Ion	Optimum dosage of ESM [g]	Adsorption time [min]	Adsorption temperature [$^{\circ}\text{C}$]
Cr(VI)	1.2	45	50
Cd(II)	1.0	30	70
Cu(II)	1.2	60	70

Table 2, the optimum experimental conditions were different for each ion.

The sorption of Cr(VI) on ESM was studied by Daraei et al. [99]. The ESM was crushed into a powder before the sorption tests. The effects of various phenomena were investigated (pH, Cr(VI) ion concentration, sorbent dosage, contact time, temperature). The experimental results were then used for theoretical calculations to measure the effect of each of the variables. The maximum removal (81.47%) was achieved at temperature 20 °C, pH 3.54, Cr(VI) ion concentration 5.0 mg l⁻¹, time 117.52 min and dosage 3.78 g.

The mechanism of Cd(II) ion sorption on ESM was studied in detail by Flores-Cano et al. [100]. Although this paper focused on the sorption ability of ESM, the ESM also contributed to the sorption potential of the material.

The composite material composed of layered double hydroxide (LDH) and ESM was synthesized as potential adsorbent for Cr(VI) ions, in which ESM serves as the substrate and template to immobilize the LDH formed by an *in situ* hydrothermal crystallization

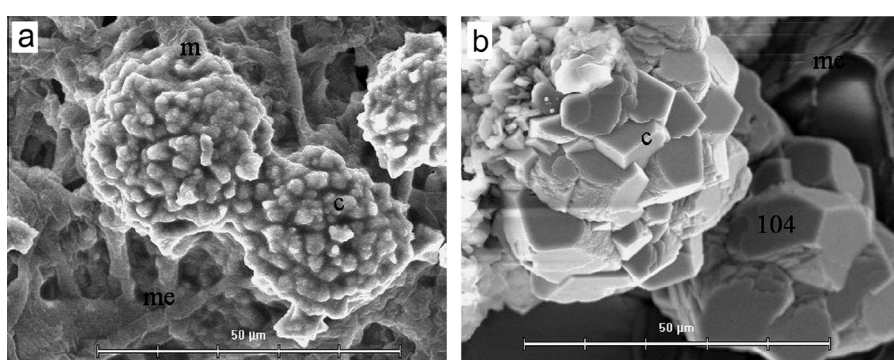


Fig. 12. Scanning electron micrographs of 5 h 30 min post-oviposition eggshell incubated for 72 h at: (a) pH 7.4 and (b) pH 9.0 (m: mammillae; me: membranes; c: calcite crystals). Modified with permission from Ref. [95].

© Copyright 2004, Elsevier.

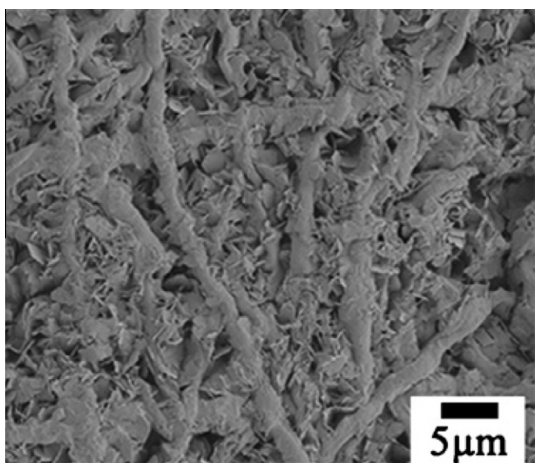


Fig. 14. SEM image of the MgAl-Cl⁻ LDH/ESM composite membrane. Reprinted with permission from Ref. [9].

[9]. The sorption properties of pure ESM and the two composite materials were compared and the effect of pH was also studied. The MgAl-Cl⁻ LDH/ESM composite membrane had the best adsorption properties among the studied materials and, moreover, the highest sorption ability was maintained even if the pH value of the Cr(VI) ion solution was not further adjusted by addition of acid, which is of practical significance in wastewater treatment. The SEM image of the MgAl-Cl⁻ LDH/ESM composite membrane is shown in Fig. 14.

Shimada et al. [101] have compared the sorption ability of ESM with that of chicken feathers by using these materials as a sorbents of precious metal ions such as Au(III), Pd(II) and Pt(IV). The adsorption capacity of ESM was higher than that of feather. Adsorption of Au(III) on the ESM was prominent at pH <5.

The sorption properties of ESM can be improved by its functionalization. Thiol-functionalized ESM was used for the removal of toxic mercury from wastewater [102]. The results indicated that the modification of ESM has greatly enhanced the adsorption capacity for Hg(II) ions, because the maximum sorption capacity increased more than 3 times in comparison with the unmodified ESM. The optimum pH for the sorption was over a wide range, 2–8, and almost complete recovery (96%) was achieved. The thiolated ESM was used also by Wang et al. [78]. In this study the potential of the material to adsorb various ions was evaluated and the results were compared with the sorption ability of non-functionalized ESM. The results showed that adsorption ability of the thiol-functionalized ESM toward Cr(VI), Hg(II), Cu(II), Pb(II), Cd(II) and Ag(I) ions improved 1.6-, 5.5-, 7.7-, 12.4-, 12.7- and 21.1-fold, respectively, in comparison with non-functionalized ESM. Thiol-functionalized ESM can be used as column packing to fabricate a column for wastewater purification.

Not only are the typical sorption properties of ESM interesting, but they can also be exploited for the determination of trace amounts of ions. The sorption and determination of trace amounts of Mn(II) and Mn(VII) ions in water was studied by Zhang et al. [104]. It was shown that ESM is suitable for this application, because the detection limit for Mn ions when applying ESM as a sorbent is only 0.0131 ng l⁻¹. ESM was used also as a solid-phase extraction (SPE) adsorbent for the separation and preconcentration in combination with inductively coupled plasma-mass spectrometry for the determination of trace gold in geological samples [105]. In both these works [104,105], the suitability of the ESM for this application was validated using certified reference materials. Polyethylenimine (PEI)-functionalized ESM was applied as SPE adsorbent of trace Cu(II) in combination with flame atomic absorption

spectrometry by Zou and Huang [106]. The functionalization showed a positive effect on the dynamic uptake capacity. The detection limit was 0.15 µg l⁻¹. The operational stability of the prepared adsorbent was confirmed and it was successfully applied for the analysis of copper in environmental water and food samples.

Another element of which trace amounts can be successfully determined by the application of ESM for SPE is arsenic. Analysis of As(V) trace ion in environmental water samples in combination with hydride generation atomic fluorescence spectrometry was successfully performed by Zhang et al. [107]. Thiolated ESM can also be utilized for trace elemental analysis, namely the determination of inorganic selenium [108]. Both Se(VI) and Se(IV) ions are adsorbed, but the first is retained reversibly, possibly via ionic interactions, while the second is reduced to Se(0) and deposited. The suitability of ESM for this application was validated by analyzing the amount of selenium in reference materials of human hair and rice. Finally, a method using a glass column packed with ESM for the preconcentration of trace Cd(II) ion in an environmental water sample prior to its monitoring by graphite furnace atomic absorption spectrometry was developed by Cheng et al. [109]. A detection limit of 0.13 ng ml⁻¹ was achieved in this case.

3.2.2. Sorption of dyes and organics, sulfonates and fluorides

ESM is also suitable for the sorption of dyes. The sorption of malachite green from its aqueous solution was studied by Chen et al. [110]. The authors achieved an adsorption capacity of 89.72 mg g⁻¹ and almost complete recovery (98.69%) of the dye.

In Ref. [111] the sorption of the organic dye eosin B on ESM was studied. The authors observed an increase in the sorption ability with temperature. At room temperature and pressure, 95% of the dye was adsorbed and an adsorption capacity 40.9 mg g⁻¹ was achieved. The sorption of dye was also the main point in Ref. [112], in which the sorption of Congo Red on ESM was studied. The optimal adsorption capacity of 112.3 mg g⁻¹ was achieved at an initial concentration 10 mg l⁻¹ and, again, almost complete (99.17%) uptake of the dye was observed. Last but not least, the sorption of the water-soluble azo dye Eriochrome T on ESM was investigated [113]. The highest recovery (95%) of the dye was obtained in acidic conditions.

The ability of ESM to capture linear alkylbenzene sulfonates (LAS) as a model of organic pollutants was studied in Ref. [114]. Under optimum conditions, the breakthrough capacities of the ESM-packed cartridge for C10–C13 LAS homologs were found to be 30, 53, 50 and 43 µg g⁻¹, respectively. The system could respond down to 0.027 ng ml⁻¹ LAS and therefore could be successfully used for the detection of residual LAS in environmental water samples. The comparison of this material with other widely used traditional adsorbents has shown that the novel material is more suitable for this application.

Lunge et al. prepared a composite of alumina and ES for the defluoridation of wastewater [11], in which ESM was included. The authors optimized the synthesis conditions, among which the ratio between ES and ESM was an important factor. The prepared composite was compared to another fluoride sorbent and was shown to offer advantages both from the adsorption and economic points of view.

3.3. ESM for biosensors

The biotemplating ability of ESM can be further enhanced for employing ESM in biosensing applications.

A biosensor based on a combination of AuNPs and immobilized enzyme glucose oxidase (GO_x) on the surface of ESM was prepared by Zheng et al. [85]. The effect of pH, buffer concentration and temperature on the properties of the sensor was also studied. This biosensor has been successfully applied to determine the glucose

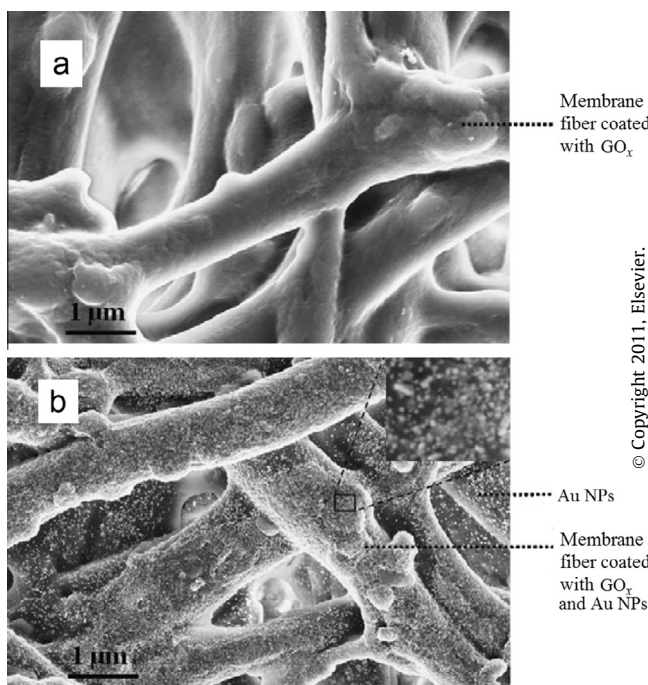


Fig. 15. SEM image of ESM (a) covered with the immobilized enzyme GO_x; (b) covered with the immobilized enzyme GO_x and AuNPs. Inset in (b) is the enlarged image of the small area of the protein fiber in the GO_x-AuNPs/ESM system. Modified with permission from Ref. [85].

concentration in human blood serum. Fig. 15 shows SEM images of ESM covered with the immobilized enzyme (GO_x/ESM) (a) and ESM covered with immobilized enzyme together with AuNPs (GO_x-AuNPs/ESM) (b) [85].

When GO_x is immobilized on the membrane fibers, they appear rougher with clusters or lumps of GO_x (Fig. 15a) as compared to the smooth fibers of pure ESM (Figs. 3c, 4a). In Fig. 15b GO_x-AuNPs/ESM with huge amount of homogeneously distributed spherical AuNPs with average sizes of ~25 nm appearing as white dots can be seen. The inset in Fig. 15b is the magnified image of the AuNPs on the ESM fiber. The fibers in this case are even rougher, because in addition to the lumps of immobilized enzyme they also contain many spherical AuNPs which cannot be leached out [85]. A very similar biosensor was developed by Zhang et al. [115]. The biosensor showed a narrower range of linear response to glucose concentration compared to the previous one; however, the detection limit of this biosensor was lower. This sensor has been shown to be useful for obtaining information about the glucose content in food. A glucose-determining biosensor with ESM was developed to measure the remaining glucose in soil samples [116]. By utilizing this sensor, it is possible to assess and compare the toxic effect of heavy metals on soil microbes. A biosensor based on the catalytic effect of platinum nanoparticles (PtNPs) has been developed by Liu et al. [117]. PtNPs were *in situ* synthesized on ESM upon which GO_x was simultaneously immobilized. This biosensor was successfully applied for the determination of glucose concentration in human blood serum. A chemiluminescence (CL) flow-through biosensor for glucose was developed by immobilizing GO_x and horseradish peroxidase on ESM with glutaraldehyde as a cross-linker [118]. This biosensor exhibited decent biosensing properties and was successfully applied to the determination of glucose in human serum. A DNAzyme-based CL biosensor for sensitive detection of hydrogen peroxide (H₂O₂) using ESM, which served as an immobilization platform for the DNAzyme, was developed in Ref. [119]. The immobilized DNAzyme was then packed into a mini-column as a CL flow cell.

Mesoporous hierarchical α-Fe₂O₃ was prepared in Ref. [120] by using ESM as a biotemplate, and due to the mesoporous hierarchical structures and high surface area, the ESM-morphic α-Fe₂O₃ material can be applied in gas sensing. It exhibited the highest selectivity and sensitivity to acetic acid among the tested gases, a rapid response and short recovery times.

An amperometric cost-effective biosensor for dopamine based on the enzyme monoamine oxidase immobilized on a glutaraldehyde-activated ESM that was deposited on a glassy carbon electrode was developed by Joshi et al. [121]. The sensor showed good characteristics necessary for the application as biosensor (shown in Table 3). The properties were further improved by coating with Nafion, after which the shelf life of the enzyme, the detection limit and the selectivity over ascorbic and uric acid was increased. Another electrochemical dopamine biosensor was developed by Tembe et al. [122] based on the immobilization of the enzyme tyrosinase on ESM using glutaraldehyde and subsequent mounting on the surface of glassy carbon electrode.

A microbial biosensor was prepared by immobilizing cells of the microorganism *Pseudomonas fluorescens* on ESM [123]. This material was fixed tightly onto the surface of a carbon paste electrode (CPE) with a silicone rubber O-ring. This sensor is able to measure the respiratory activity of the cells by determining the amount of consumed oxygen. The authors have also tuned the biosensor by utilizing ferrocene. Another microbial biosensor based on ESM is capable of determining ethanol content [124]. It comprises a *Methylobacterium organophilum*-immobilized ESM and an oxygen electrode. The biosensor was successfully applied to determine the amounts of ethanol in various samples of alcohol and the obtained results are comparable to that obtained by gas chromatography.

Finally, an ESM-based potentiometric urea biosensor was developed by D'Souza et al. [125]. Urease was immobilized on PEI-treated ESM through adsorption. Immobilized membrane was associated with an ammonium-ion-selective electrode. In Fig. 16, the SEM image shows the fibers and cavities of the ESM being occupied with PEI and urease enzyme after immobilization, which confirms the success of the immobilization of the urease on the surface of the ESM.

The most important characteristics of synthesized biosensors based on ESM are shown in Table 3.

The biosensing potential can also be utilized in the field of immunoassays. A novel ESM-based immunosensor for determining human immunoglobulin M (H IgM) in serum was developed by Tang et al. [125]. The immunosensor was fabricated by immobilizing goat anti-human IgM antibody on ESM with glutaraldehyde. Based on the immunoreactions of goat anti-human IgM (primary antibody), H IgM (target antigen) and the goat anti-human IgM (secondary antibody), a sandwich complex was formed on the ESM, and FITC-labeling secondary antibody could be employed to

Table 3
Various sensing characteristics of synthesized biosensors on the basis of ESM.

Sensor for	Response time [s]	Detection limit [μM]	Linear working range [μM]	Ref.
Glucose	<30	3.50	8.33–966	[85]
Glucose	<60	2.5	5–525	[115]
Glucose	60	0.5	1–100	[118]
Glucose	<30	5	10–225	[117]
Hydrogen peroxide	60	0.05	0.1–10	[119]
Acetic acid	18	50		[120]
Dopamine	5–10	20	50–250	[121]
Dopamine		25	50–250	[122]
Oxygen	100	25	60–750	[123]
Ethanol	100	25	0.05–75	[124]
Urea	120	100	0.5–10	[125]

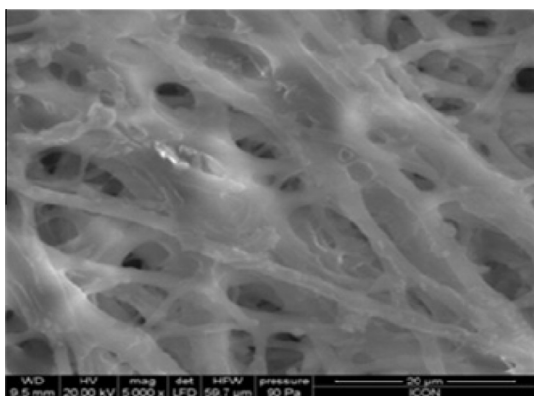


Fig. 16. SEM image of immobilized urease on PEI-treated ESM. Reprinted with permission from Ref. [125].

detect the target antigen. Under optimized conditions, the linear range for determining HlgM is 5–60 ng ml⁻¹ and the detection limit is 4.3 ng ml⁻¹. The biocompatible sensor exhibited remarkable storage stability, permeability and offered excellent fluorescence response to HlgM. The new biosensor provides an alternative to determine antigens and other bioactive molecules. The experimental procedure for the sandwich immunoassay immobilized on ESM is shown in Fig. 17 [103].

3.4. ESM in medicine

In addition to the wide variety of applications in the field of materials science, ESM can also be utilized in other spheres, e.g. medicine. Its use as a biological dressing for burnt skin has been noted [126]. This aspect was reviewed in [127], where the potential of other biomaterials for this particular application was also discussed.

Today, some medical researchers are using Natural Eggshell Membrane (NEM[®]), a commercial product of ESM Technologies LLC, Carthage, MO, USA. Ruff et al. [128] studied the potential of

NEM[®] as a possible new effective and safe therapeutic option for the treatment of pain and inflexibility associated with JCT disorders. It was shown that daily supplementation with 500 mg NEM[®] reduced pain significantly—both rapidly (7 days) and continuously (30 days). In another work [129], a clinical study was conducted to evaluate the efficiency and safety of NEM[®] as a therapeutic for pain and stiffness associated with osteoarthritis of the knee. Again, the results were satisfactory, because after supplementation with NEM[®] (500 mg taken once daily), significantly reduced joint pain and stiffness was observed. The potential of NEM[®] as an anti-inflammatory product was documented by Benson et al. [130].

ESM has also found application in ophthalmology—a cheap and versatile eye model was developed for use during vitreous surgery training [131]. It can be used for simulating the spatial recognition of the vitreous chamber.

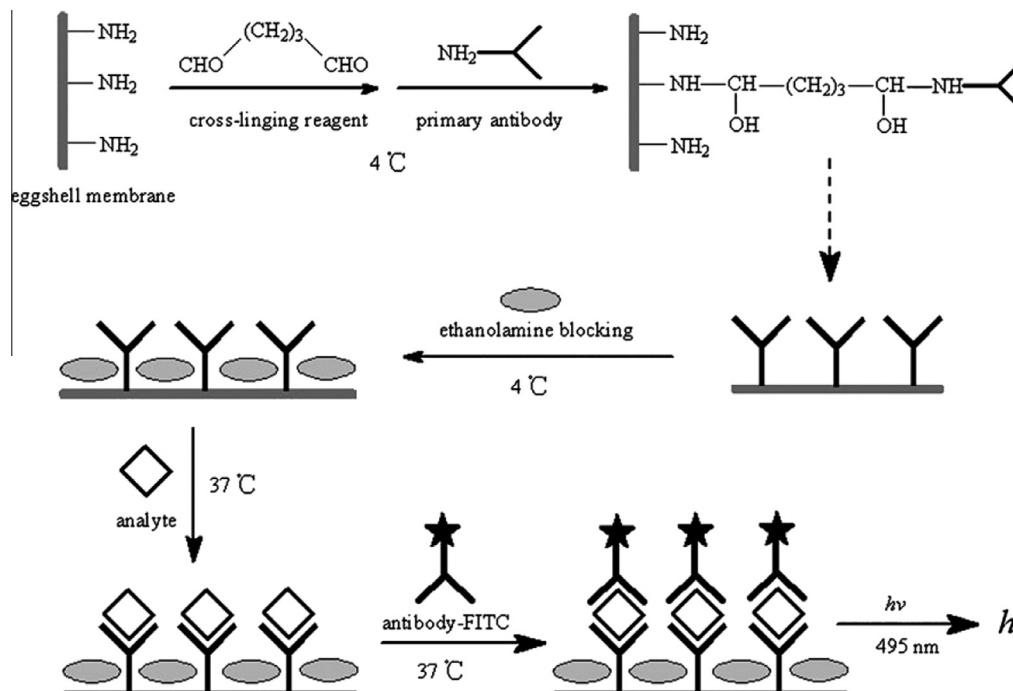
The positive effect of ESM was also observed in a study dealing with the final outcome of nerve regeneration [132]. It was concluded that ESM effectively enhances nerve regeneration and promotes functional recovery in injured nerves.

Mucoadhesive microspheres loaded with the antiviral drug acyclovir were prepared for the purpose of improving the oral bioavailability of acyclovir [133]. ESM was used to substitute the animal stomach mucosa in this experiment.

3.5. Other utilization of ESM

Older works have noted the antibacterial activity of ESM. In the work by Poland et al. [134], antibacterial activity of ESM against various types of bacteria, including *Escherichia coli*, was studied. The results showed the potential ability of ESM to alter bacterial heat resistance. The ability of ESM proteins to interact and disrupt the membrane integrity of bacteria was proven in Ref. [135].

ESM has also been used in electrochemistry. Porous nanospheres of NiO 5–10 nm in size were synthesized with the help of ESM in Ref. [136]. The product exhibited good capacitive performance of 550 F g⁻¹ at a current density of 1 A g⁻¹. Li et al. [137] have studied the electrochemical properties of carbonized ESM.



© Copyright 2011, Springer.

Fig. 17. The experimental flowsheet for sandwich immunoassay immobilized on ESM. Reprinted with permission from Ref. [103].

3-D macroporous carbon film composed of interwoven carbon fibers containing ~10% oxygen and ~8% nitrogen was formed. Excellent electrochemical characteristics (specific capacitances of 297 and 284 F g⁻¹ in alkaline and acidic electrolytes, respectively) were achieved in a three-electrode system and a capacity loss of only 3% after 10,000 cycles was observed. Carbonized ESM was recently tested as a battery material, namely as a natural polysulfide reservoir for highly reversible Li-S batteries [138].

ESM has also been used as a separator in supercapacitor, where it was utilized as a membrane between two parts of the electrolyser [139]. The porous structure, high temperature of decomposition (over 200 °C), low water uptake, low swelling property and good mechanical properties make ESM a potential material for supercapacitors. The newly synthesized material exhibited better properties than polyethylene separators.

ESM can also be utilized for the synthesis of hydroxyapatite (HAp). Neelakandeswari et al. [140] synthesized HAp from its precursors (calcium chloride dihydrate and diammonium hydrogen phosphate). ESM was used as a "membrane" for the controlled diffusion of phosphate ions towards calcium ions, due to which further nucleation and crystal growth of HAp was possible. The authors studied the influence of pH on the morphology of hexagonal HAp. They found out that with an increase in pH, the "needle-like" particles change their shape into the "rice-shaped" ones and that the lattice parameters also change (the size in the direction *a* increases, though the size in the direction *c* remains constant) [140].

Carbon nanodots (C-dots) are interesting material as a potential substitute for semiconductor quantum dots which are widely used as a fluorescent entities in medicine. The main advantage of C-dots is their lower toxicity. Wang et al. [141] have used ESM ash as a source of carbon for the synthesis of the water-soluble C-dots in a microwave oven. The maximal fluorescent peak was located at 450 nm and the quantum yield was 14%.

Very recently, the potential of ESM to serve not only as a template, but directly as a source of sulfur for sulfide semiconductor

nanocrystals was demonstrated in Ref. [142]. Using principles of mechanochemistry [143,144], the authors obtained nanocrystalline lead sulfide embedded in the ESM matrix (Fig. 18).

The outer ESM was utilized as a part of a new type of delivery system, in which it was combined with emulsified polysaccharide/protein microcapsules incorporated with vitamin E [145]. The synthesized system exhibited better controlled release properties than the microcapsules alone because of the steric blocking effect. In addition, when the system was formed by utilizing pectin/protein as wall material, it showed more resistance against enzymatic attack.

Trimbos et al. pursued the possible utilization of ESM in the field of ornithology [146]. The usefulness of ESM as a DNA source for population genetic research was studied. The DNA comes from the adjacent blood vessels that adhere to ESM in hatched egg fragments. Therefore, DNA of hatchlings can be obtained and used for wild bird population studies. The results showed that genetic information stored within ESM DNA in comparison with blood DNA was not affected by degeneration or possible cross-contamination. Therefore it can be claimed that ESM can be used for population genetic research.

3.6. Utilization of SEP

As was mentioned earlier, although ESM is a unique natural structure applicable in various areas, some of its applications are limited due to its insolubility. This problem was overcome by the preparation of SEP [62]. Later, the structure, morphology and biocompatibility of SEP was studied in detail [63]. In 2007, the antibacterial activity and biodegradability of SEP was studied by the same group [147]. The authors found out that in contrast to natural ESM, SEP does not possess antibacterial property against *E. coli*. Biodegradation tests with trypsin showed that both ESM and SEP are biodegradable.

Protein-based electrospun nanofibers have specific properties that make them suitable for mimicking the scaffolds of human skin

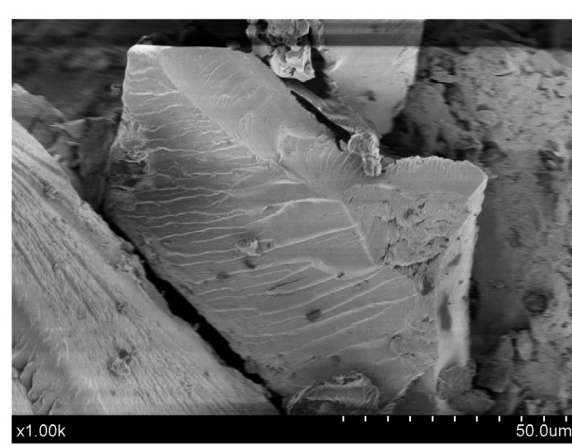
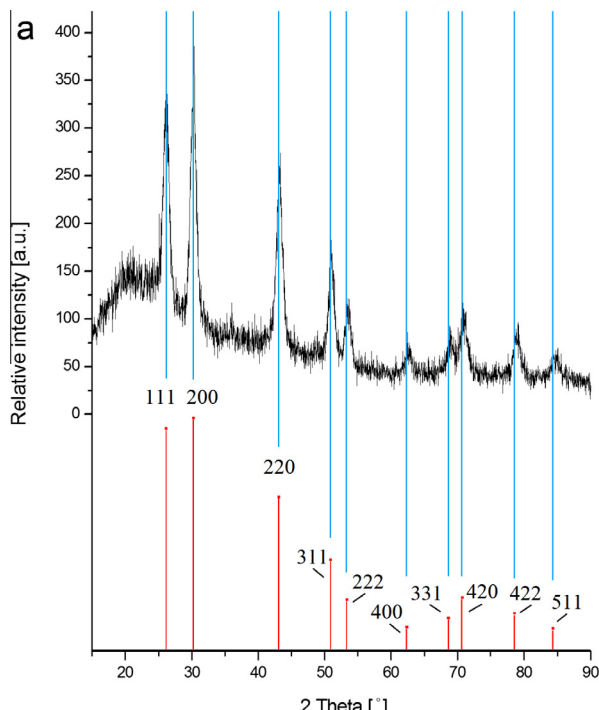


Fig. 18. Mechanochimically synthesized lead sulfide using eggshell membrane: (a) XRD pattern (blue lines correspond to the reflections of the planes of crystalline PbS); (b) SEM image of the particle obtained after 180 min of milling. Reprinted with permission from Ref. [142].

tissue in biomedical applications—this is called guided tissue regeneration (GTR). However, toxic organic solvents are generally used for the process. Two biocompatible polymers, poly(ethylene oxide) and poly(vinyl alcohol), were used to improve the processability of SEP for electrospinning applications in aqueous media [148]. The insoluble processable fibers were prepared by treatment with catechin and no toxic solvent was required for the process. The obtained fibers could be potentially applied as wound dressings or as cosmetic sheets. Improving the electrospinning properties of SEP was also the focus of Ref. [149]. SEP was co-extruded with biocompatible poly(ϵ -caprolactone) (PCL). The SEP/PCL was fabricated into a micro/nanofiber web, which showed increased hydrophilic and tensile properties relative to a pure PCL web. The objective of Ref. [150] was to prepare and evaluate a new type of SEP/poly(lactic-co-glycolic acid) (PLGA) nanofiber using an electrospinning method for GTR membrane application. The mechanical properties of SEP can be greatly improved by the addition of PLGA. A biological study done on L-929 fibroblast cells showed that SEP/PLGA nanofibers could enhance cell attachment, spreading and proliferation. The study indicated the potential of SEP/PLGA nanofibers for GTR application and provided a basis for future optimization. SEP was successfully immobilized on poly(D,L-lactic acid) (PDLLA) membrane surface by a physical entrapment method to enhance its cytocompatibility [151]. A study of the proliferation of cell culture of NIH3T3 fibroblasts showed that the SEP-modified PDLLA membrane has much enhanced cytocompatibility in comparison with virgin PDLLA membrane. The same effect was observed in case of chitosan, the biocompatibility of which can also be improved by interaction with SEP [152]. Moreover, the mechanical properties of SEP (tensile strength and elongation at break increase) can be improved with an increase in chitosan content. In another similar study [153], SEP was co-electrospun with biodegradable synthetic polymers poly(propylene carbonate) (PPC) and poly(lactic acid) (PLA) in various proportions from 1,1,1,3,3-hexafluoro-2-propanol solutions. The aim was to prepare fibrous scaffolds having simultaneously good mechanical properties and biocompatibility. Evaluation of the mechanical properties showed that both the tensile strength and elongation at break increase with increasing incorporation of both polymers. The biocompatibility of PPC/SEP and PLA/SEP blend fibrous scaffolds was also studied on the NIH3T3 cell culture. Similarly in this case, the biocompatibility was improved significantly in comparison with fibrous scaffolds composed of pure PPC or PLA.

The potential of SEP to be a new alternative in the production of antioxidative peptides was investigated in Ref. [154]. Five proteases were employed as hydrolytic enzymes for the preparation of antioxidative peptides from SEP, and the antioxidative activities of the hydrolysates were investigated using a chemiluminescence method. The results have confirmed that the material could be a new alternative in the production of antioxidative peptides.

Quite recently, Sah and Pramanik utilized SEP to modify porous silk fibroin (SF) scaffold in order to improve the cell affinity properties of the scaffold for tissue regeneration [155]. A significant improvement in the cell adhesion and proliferation of mesenchymal stem cells on the SF scaffold was achieved after its modification with SEP. In addition, the cytocompatibility of the material was confirmed.

4. Conclusion

ESM represents very interesting natural biomaterial with a unique structure. As was demonstrated within this review article, due to its properties, ESM can be applied in very wide range of applications, including as biotemplates, biosorbents, biosensors or in medicine.

However, some drawbacks must be noted. Some applications of ESM are limited and it has to be modified to be usable (e.g. SEP or thiolated ESM has to be used). Moreover, ESM has to be separated from ES after the production of eggs, which complicates its application on an industrial scale.

Nevertheless, ESM is a widely studied material nowadays and new potential applications are still emerging. Even taking into account the above-mentioned drawbacks, it would be a mistake not to utilize its advantages as a unique natural biomaterial in future research activities both in the laboratory and on an industrial scale.

Acknowledgements

This work was supported by projects of the Agency for Science and Development (APVV-0189-10), the Slovak Grant Agency (VEGA 2/0027/13) and the Slovak Academy of Sciences (SAS Centre of Excellence: CFNT-MVEP). The support of the European Regional Fund (projects nanoCEXmat I- ITMS 26220120019 and nanoCEXmat II- ITMS 26220120035 is also gratefully acknowledged.

Appendix A. Figures with essential color discrimination

Certain figures in this article, particularly Figs. 1, 2, 5, 9, 10, and 18, are difficult to interpret in black and white. The full color images can be found in the on-line version, at <http://dx.doi.org/10.1016/j.actbio.2014.03.020>.

References

- [1] King'ori AM. A review of the uses of poultry eggshells and shell membranes. *Int J Poult Sci* 2011;10:908–12.
- [2] Guru PS, Dash S. Sorption on eggshell waste—A review on ultrastructure, biominerilization and other applications. *Adv Colloid Interface Sci* 2014;9:90. in press, <http://dx.doi.org/10.1016/j.cis.2013.12.013>.
- [3] Robinson DS, King NR. Carbonic anhydrase and formation of the hen's egg shell. *Nature* 1963;199:497–8.
- [4] Osuji CI. Acid glycosaminoglycan of eggshell membranes. *BBA - Gen Subjects* 1971;244:481–3.
- [5] Wu TM, Rodriguez JP, Fink DJ, Carrino DA, Blackwell J, Caplan AI, et al. Crystallization studies on avian eggshell membranes—Implications for the molecular factors controlling eggshell formation. *Matrix Biol* 1995;14:507–13.
- [6] Devi PS, Banerjee S, Chowdhury SR, Kumar GS. Eggshell membrane: a natural biotemplate to synthesize fluorescent gold nanoparticles. *RSC Adv* 2012;2:11578.
- [7] Zhou J, Wang S, Nie F, Feng L, Zhu G, Jiang L. Elaborate architecture of the hierarchical hen's eggshell. *Nano Res* 2010;4:171–9.
- [8] Kumari TSD, Kumar TP. Synthesis of macroporous LiMn₂O₄ with avian egg membrane as a template. *Ionics* 2010;16:61–6.
- [9] Guo XX, Zhang FZ, Peng Q, Xu SL, Lei XD, Evans DG, et al. Layered double hydroxide/eggshell membrane: An inorganic biocomposite membrane as an efficient adsorbent for Cr(VI) removal. *Chem Eng J* 2011;166:81–7.
- [10] Ishikawa S, Suyama K, Arihara K, Itoh M. Uptake and recovery of gold ions from electroplating wastes using eggshell membrane. *Bioresour Technol* 2002;81:201–6.
- [11] Lunge S, Thakre D, Kamble S, Labhsetwar N, Rayalu S. Alumina supported carbon composite material with exceptionally high defluoridation property from eggshell waste. *J Hazard Mater* 2012;237:161–9.
- [12] Xu Z, Neoh KG, Kishen A. A biomimetic strategy to form calcium phosphate crystals on type I collagen substrate. *Mater Sci Eng C* 2010;30:822–6.
- [13] Su H, Han J, Wang N, Dong Q, Zhang D, Zhang C. In situ synthesis of lead sulfide nanoclusters on eggshell membrane fibers by an ambient bio-inspired technique. *Smart Mater Struct* 2008;17:015045.
- [14] Su H, Wang N, Dong Q, Zhang D. Incubating lead selenide nanoclusters and nanocubes on the eggshell membrane at room temperature. *J Membr Sci* 2006;283:7–12.
- [15] Su H, Xu J, Chen JJ, Moon WJ, Zhang D. In situ formation and assembly of CdS nanocrystallites into polyhedrons on eggshell membrane at room temperature. *Appl Phys A* 2012;106:93–7.
- [16] Ponkham W, Limroongreungrat K, Sangnark A. Extraction of collagen from hen eggshell membrane by using organic acids. *Thai J Agr Sci* 2011;44:354–60.
- [17] Su H, Song F, Dong Q, Li TQ, Zhang X, Zhang D. Bio-inspired synthesis of ZnO polyhedral single crystals under eggshell membrane direction. *Appl Phys A* 2011;104:269–74.

- [18] Torres FG, Troncoso OP, Piaggio F, Hijar A. Structure-property relationships of a biopolymer network: The eggshell membrane. *Acta Biomater* 2010;6:3687–93.
- [19] Li N, Niu LN, Qi YP, Yiu CKY, Ryou H, Arola DD, et al. Subtleties of biominerisation revealed by manipulation of the eggshell membrane. *Biomaterials* 2011;32:8743–52.
- [20] Lee T, Chang SC, Peng JF. Tris(8-hydroxyquinoline)aluminum (III) (Alq3) nanowires templated from an eggshell membrane. *Thin Solid Films* 2010;518:5488–93.
- [21] Dong Q, Su H, Zhang C, Zhang D, Guo Q, Kiessling F. Fabrication of hierarchical ZnO films with interwoven porous conformations by a bioinspired templating technique. *Chem Eng J* 2008;137:428–35.
- [22] Yoo S, Hsieh JS, Zou P, Kokoszka J. Utilization of calcium carbonate particles from eggshell waste as coating pigments for ink-jet printing paper. *Bioresour Technol* 2009;100:6416–21.
- [23] Arias JL, Fink DJ, Xiao SQ, Heuer AH, Caplan AI. Biominerization and eggshells: cell-mediated acellular compartments of mineralized extracellular matrix. *Int Rev Cytol* 1993;145:217–50.
- [24] Nys Y, Gautron J, García-Ruiz JM, Hincke MT. Avian eggshell mineralization: biochemical and functional characterization of matrix proteins. *Comptes Rendus Palevol* 2004;3:549–62.
- [25] Hincke MT, Nys Y, Gautron J, Mann K, Rodriguez-Navarro AB, McKee MD. The eggshell: structure, composition and mineralization. *Front Biosci (Landmark Ed)* 2012;17:1266–80.
- [26] Lee SM, Grass G, Kim GM, Dresbach C, Zhang LB, Gosele U, et al. Low-temperature ZnO atomic layer deposition on biotemplates: flexible photocatalytic ZnO structures from eggshell membranes. *Phys Chem Chem Phys* 2009;11:3608–14.
- [27] Bellairs R, Boyde A. Scanning electron microscopy of the shell membranes of the hen's egg. *Z Zellforsch Mikrosk Anat* 1969;96:237–49.
- [28] Liang JWW, Frank JF, Bailey S. Visualization of eggshell membranes and their interaction with *Salmonella enteritidis* using confocal scanning laser microscopy. *J Food Prot* 1997;60:1022–8.
- [29] Hincke MT, Nys Y, Gautron J. The role of matrix proteins in eggshell formation. *J Poult Sci* 2010;47:208–19.
- [30] Hincke MT, Gautron J, Panheleux M, Garcia-Ruiz J, McKee MD, Nys Y. Identification and localization of lysozyme as a component of eggshell membranes and eggshell matrix. *Matrix Biol* 2000;19:443–53.
- [31] Arias JL, Cataldo M, Fernandez MS, Wu JJ, Kessi E. Effect of beta-aminopropionitrile on the eggshell mineralisation. *Br Poult Sci* 1997;38:351–6.
- [32] Chowdhury SD. Shell membrane-protein system in relation to lathyrone toxicity and copper deficiency. *Worlds Poult Sci J* 1990;46:153–69.
- [33] Leach RM. Biochemistry of the organic matrix of the eggshell. *Poult Sci* 1982;61:2040–7.
- [34] Kawewong K, Garnjanagoonchorn W, Jirapakkul W, Roytrakul S. Solubilization and identification of hen eggshell membrane proteins during different times of chicken embryo development using the proteomic approach. *Protein J* 2013;32:297–308.
- [35] Arias JL, Fernandez MS, Dennis JE, Caplan AI. Collagens of the chicken eggshell membranes. *Connect Tissue Res* 1991;26:37–45.
- [36] Fernandez MS, Araya M, Arias JL. Eggshells are shaped by a precise spatio-temporal arrangement of sequentially deposited macromolecules. *Matrix Biol* 1997;16:13–20.
- [37] Harris ED, Blount JE, Leach RM. Localization of lysyl oxidase in hen oviduct: implications in egg shell membrane formation and composition. *Science* 1980;208:55–6.
- [38] Wong M, Hendrix MJ, von der Mark K, Little C, Stern R. Collagen in the egg shell membranes of the hen. *Dev Biol* 1984;104:28–36.
- [39] Zhao YH, Chi YJ. Characterization of collagen from eggshell membrane. *Biotechnology* 2009;8:254–8.
- [40] Mann K, Olsen JV, Macek B, Gnad F, Mann M. Phosphoproteins of the chicken eggshell calcified layer. *Proteomics* 2007;7:106–15.
- [41] D'Ambrosio C, Arena S, Scaloni A, Guerrier L, Boschetti E, Mendieta ME, et al. Exploring the chicken egg white proteome with combinatorial peptide ligand libraries. *J Proteome Res* 2008;7:3461–74.
- [42] Farinazzo A, Restuccia U, Bachì A, Guerrier L, Fortis F, Boschetti E, et al. Chicken egg yolk cytoplasmic proteome, mined via combinatorial peptide ligand libraries. *J Chromatogr A* 2009;1216:1241–52.
- [43] Mann K. The chicken egg white proteome. *Proteomics* 2007;7:3558–68.
- [44] Mann K, Mann M. The chicken egg yolk plasma and granule proteomes. *Proteomics* 2008;8:178–91.
- [45] Mann K. Proteomic analysis of the chicken egg vitelline membrane. *Proteomics* 2008;8:2322–32.
- [46] Arias JL, Nakamura O, Fernandez MS, Wu JJ, Knigge P, Eyre DR, et al. Role of type X collagen on experimental mineralization of eggshell membranes. *Connect Tissue Res* 1997;36:21–33.
- [47] Wang X, Ford BC, Praul CA, Leach RM. Collagen X expression in oviduct tissue during the different stages of the egg laying cycle. *Poult Sci* 2002;81:805–8.
- [48] Gautron J, Hincke MT, Panheleux M, Garcia-Ruiz JM, Boldicke T, Nys Y. Ovotransferrin is a matrix protein of the hen eggshell membranes and basal calcified layer. *Connect Tissue Res* 2001;42:255–67.
- [49] Hincke MT. Ovalbumin is a component of the chicken eggshell matrix. *Connect Tissue Res* 1995;31:227–33.
- [50] Gautron J, Murayama E, Vignal A, Morisson M, McKee MD, Rehault S, et al. Cloning of ovocalyxin-36, a novel chicken eggshell protein related to lipopolysaccharide-binding proteins, bactericidal permeability-increasing proteins, and plunc family proteins. *J Biol Chem* 2007;282:5273–86.
- [51] Cordeiro CMM, Esmaili H, Ansah G, Hincke MT. Ovocalyxin-36 is a pattern recognition protein in chicken eggshell membranes. *PLoS ONE* 2013;8:e84112.
- [52] Starcher BC, King GS. The presence of desmosine and isodesmosine in eggshell membrane protein. *Connect Tissue Res* 1980;8:53–5.
- [53] Nys Y, Gautron J, McKee MD, Garcia-Ruiz JM, Hincke T. Biochemical and functional characterisation of eggshell matrix proteins in hens. *Worlds Poult Sci J* 2001;57:401–13.
- [54] Gautron J, Nys Y. Eggshell Matrix Proteins. In: Huopalahti R, López-Fandino R, Anton M, Schade R, editors. *Bioactive Egg Compounds*. Berlin: Springer Verlag; 2007. p. 103–8.
- [55] Picard J, Paul-Gardais A, Vedel M. Sulfated glycoproteins from egg shell membranes and hen oviduct. Isolation and characterization of sulfated glycopeptides. *Biochim Biophys Acta* 1973;320:427–41 [in French].
- [56] Yamauchi K, Manabe N, Matsumoto Y, Yamauchi K. Increased collagen accumulation in eggshell membrane after feeding with dietary wood charcoal powder and vinegar. *Connect Tissue Res* 2013;54:416–25.
- [57] Carrino DA, Dennis JE, Wu TM, Arias JL, Fernandez MS, Rodriguez JP, et al. The avian eggshell extracellular matrix as a model for biominerization. *Connect Tissue Res* 1996;35:325–8.
- [58] Nakano T, Ikawa NI, Ozimek L. Chemical composition of chicken eggshell and shell membranes. *Poult Sci* 2003;82:510–4.
- [59] Kodali VK, Gannon SA, Paramasivam S, Raje S, Polenova T, Thorpe C. A novel disulfide-rich protein motif from avian eggshell membranes. *PLoS ONE* 2011;6.
- [60] Wang XJ, Li Q, Yuan Y, Mei B, Huang R, Tian Y, et al. New method for effectively and quantitatively labeling cysteine residues on chicken eggshell membrane. *Org Biomol Chem* 2012;10:8082–6.
- [61] Takahashi K, Shirai K, Kitamura M, Hattori M. Soluble egg shell membrane protein as a regulating material for collagen matrix reconstruction. *Biosci Biotechnol Biochem* 1996;60:1299–302.
- [62] Yi F, Yu J, Guo ZX, Zhang LX, Li Q. Natural bioactive material: a preparation of soluble eggshell membrane protein. *Macromol Biosci* 2003;3:234–7.
- [63] Yi F, Guo Z-X, Zhang L-X, Yu J, Li Q. Soluble eggshell membrane protein: preparation, characterization and biocompatibility. *Biomaterials* 2004;25:4591–9.
- [64] Rath MK, Choi BH, Ji MJ, Lee KT. Eggshell-membrane-templated synthesis of hierarchically-ordered NiO-Ce_{0.8}Gd_{0.2}O_{1.9} composite powders and their electrochemical performances as SOFC anodes. *Ceram Int* 2014;40:3295–304.
- [65] Weymuth T, Jacob CR, Reiher M. A local-mode model for understanding the dependence of the extended amide III vibrations on protein secondary structure. *J Phys Chem B* 2010;114:10649–60.
- [66] Kaiden K, Matsui T, Tanaka S. A study of the amide-III band by FT-IR spectrometry of the secondary structure of albumin, myoglobin, and gamma-globulin. *Appl Spectrosc* 1987;41:180–4.
- [67] Dong Q, Su H, Zhang D, Cao W, Wang N. Biogenic synthesis of tubular SnO₂ with hierarchical intertextures by an aqueous technique involving glycoprotein. *Langmuir* 2007;23:8108–13.
- [68] Bandekar J. Amide modes and protein conformation. *Biochim Biophys Acta* 1992;1120:123–43.
- [69] Arami M, Limae NY, Mahmoodi NM. Investigation on the adsorption capability of egg shell membrane towards model textile dyes. *Chemosphere* 2006;65:1999–2008.
- [70] Kong J, Yu S. Fourier transform infrared spectroscopic analysis of protein secondary structures. *Acta Biochim Biophys Sin* 2007;39:549–59.
- [71] Tsai WT, Yang JM, Lai CW, Cheng YH, Lin CC, Yeh CW. Characterization and adsorption properties of eggshells and eggshell membrane. *Bioresour Technol* 2006;97:488–93.
- [72] Hsieh S, Chou HH, Hsieh CW, Wu DC, Kuo CH, Lin FH. Hydrogen peroxide treatment of eggshell membrane to control porosity. *Food Chem* 2013;141:2117–21.
- [73] Gunasekaran S, Sailatha E. Vibrational analysis of pyrazinamide. *Indian J Pure Appl Phys* 2008;46:315–20.
- [74] Liu D, Li YG, Xu H, Sun SQ, Wang ZT. Differentiation of the root of cultivated ginseng, mountain cultivated ginseng and mountain wild ginseng using FT-IR and two-dimensional correlation IR spectroscopy. *J Mol Struct* 2008;883:228–35.
- [75] Whitehead KA, Benson PS, Verran J. The detection of food soils on stainless steel using energy dispersive X-ray and Fourier transform infrared spectroscopy. *Biofouling* 2011;27:907–17.
- [76] Torres FG, Troncoso OP, Montes MR. The effect of temperature on the mechanical properties of a protein-based biopolymer network. The eggshell membrane. *J Therm Anal Calorim* 2013;111:1921–5.
- [77] Oda J, Sakai S, Kemmochi S. Mechanical evaluations of structural and material composition of eggshell. *JSME Int J A* 1998;41:121–6.
- [78] Wang S, Wei MH, Huang YM. Biosorption of multifold toxic heavy metal ions from aqueous water onto food residue eggshell membrane functionalized with ammonium thioglycolate. *J Agric Food Chem* 2013;61:4988–96.
- [79] Cheng X, Liu J, Gao Z, Xiong J, Lu D. Adsorption removal of cadmium (II) from aqueous solution by using modified eggshell membrane. 5th international Conference on Bioinformatics and Biomedical Engineering (iCBBE 2011); 2011.

- [80] Shao CY, Yuan B, Wang HQ, Zhou QA, Li YL, Guan YF, et al. Eggshell membrane as a multimodal solid state platform for generating fluorescent metal nanoclusters. *J Mater Chem* 2011;21:2863–6.
- [81] Cheng XZ, Cheng K, Liu J, Sun XF. Synthesis and characterizations of nanoparticle sulfur using eggshell membrane as template. *Mater Sci Forum* 2011;675–677:279–82.
- [82] Tang QW, Wu JH, Tang ZY, Li Y, Lin JM, Huang ML. Flexible and macroporous network-structured catalysts composed of conducting polymers and Pt/Ag with high electrocatalytic activity for methanol oxidation. *J Mater Chem* 2011;21:13354–64.
- [83] Tang QW, Tang ZY, Wu JH, Lin JM, Huang ML. A facile route to a macroporous silver network for methanol oxidation. *RSC Adv* 2011;1:1453–6.
- [84] Ashraf S, Khalid ZM, Hussain I. Eggshell membrane-templated porous gold membranes using nanoparticles as building blocks. *J Chem Soc Pak* 2013;35:730–6.
- [85] Zheng BZ, Xie SP, Qian L, Yuan HY, Xiao D, Choi MMF. Gold nanoparticles-coated eggshell membrane with immobilized glucose oxidase for fabrication of glucose biosensor. *Sensors Actuators B: Chem* 2011;152:49–55.
- [86] Liang M, Su R, Qi W, Yu Y, Wang L, He Z. Synthesis of well-dispersed Ag nanoparticles on eggshell membrane for catalytic reduction of 4-nitrophenol. *J Mater Sci* 2014;49:1639–47.
- [87] Dong Q, Su HL, Song F, Zhang D, Wang N. Hierarchical metal oxides assembled by nanocrystallites via a simple bio-inspired route. *J Am Ceram Soc* 2007;90:376–80.
- [88] Mallampati R, Valiyaveettil S. Simple and efficient biomimetic synthesis of Mn₃O₄ hierarchical structures and their application in water treatment. *J Nanosci Nanotechnol* 2012;12:618–22.
- [89] Camaratta R, Lima ANC, Reyes MD, Hernandez-Fenollosa MA, Messana JO, Bergmann CP. Microstructural evolution and optical properties of TiO₂ synthesized by eggshell membrane templating for DSSCs application. *Mater Res Bull* 2013;48:1569–74.
- [90] Pourmortazavi SM, Taghdiri M, Samimi N, Rahimi-Nasravadi M. Eggshell bioactive membrane assisted synthesis of barium tungstate nanoparticles. *Mater Lett* 2014;121:5–7.
- [91] Dong DH, Wu YZ, Zhang XY, Yao JF, Huang Y, Li D, et al. Eggshell membrane-templated synthesis of highly crystalline perovskite ceramics for solid oxide fuel cells. *J Mater Chem* 2011;21:1028–32.
- [92] Wang Z, Shao X, Larcher A, Xie K, Dong D, Li C-Z. A study on carbon formation over fibrous NiO/CeO₂ nanocatalysts during dry reforming of methane. *Catal Today* 2013;216:44–9.
- [93] Wang Z, Shao X, Hu X, Parkinson G, Xie K, Dong DH, et al. Hierarchically structured NiO/CeO₂ nanocatalysts templated by eggshell membranes for methane steam reforming. *Catal Today* 2014. in press, <http://dx.doi.org/10.1016/j.cattod.2014.01.006>.
- [94] Liu S, Que R, Wu XL. Biomembrane derived porous carbon film supported Au nanoparticles for highly reproducible surface-enhanced Raman scattering. *Anal Methods* 2013;5:5154–60.
- [95] Fernandez MS, Passalacqua K, Arias JL, Arias JL. Partial biomimetic reconstitution of avian eggshell formation. *J Struct Biol* 2004;148:1–10.
- [96] Armitage OE, Strange DGT, Oyen ML. Biomimetic calcium carbonate-gelatin composites as a model system for eggshell mineralization. *J Mater Res* 2012;27:3157–64.
- [97] Chien YC, Hincke MT, Vali H, McKee MD. Ultrastructural matrix-mineral relationships in avian eggshell, and effects of osteopontin on calcite growth in vitro. *J Struct Biol* 2008;163:84–99.
- [98] Liu N, Liu Y, Luan Y, Hu X. The elimination of heavy metal-containing wastewater by eggshells membrane. *Appl. Mech Mater* 2013;299:207–10.
- [99] Daraei H, Mittal A, Mittal J, Kamali H. Optimization of Cr(VI) removal onto biosorbent eggshell membrane: experimental & theoretical approaches. *Desalin Water Treat* 2013. in press, <http://dx.doi.org/10.1080/19442884.2013.787374>.
- [100] Flores-Cano JV, Leyva-Ramos R, Mendoza-Barron J, Guerrero-Coronado RM, Aragon-Pina A, Labrada-Delgado CJ. Sorption mechanism of Cd(II) from water solution onto chicken eggshell. *Appl Surf Sci* 2013;276:682–90.
- [101] Shimada Y, Niide T, Kubota F, Kamiya N, Goto M. Selective separation of precious metals using biomass materials. *Kagaku Kogaku Ronbun* 2010;36:255–8.
- [102] Cheng XZ, Hu CJ, Cheng K, Wei BM, Hu SC. Removal of mercury from wastewater by adsorption using thiol-functionalized eggshell membrane. *Adv Mater Res* 2010;113–116:22–6.
- [103] Tang JL, Han L, Yu YH, Kang J, Zhang YH. Studies of fluorescence immunosensor using eggshell membrane as immobilization matrix. *J Fluoresc* 2011;21:339–46.
- [104] Zhang RH, Yang XL, Liu J, Cheng XZ. Eggshell membrane biomaterials for adsorption and determination of Mn(II, VII) in environmental water. *Adv Mater Res* 2012;457–458:536–9.
- [105] Cheng XZ, Liu J, Yang XL, Chen HM, Wang YR. Eggshell membrane microcolumn solid-phase extraction and determination of trace gold in geological samples by inductively coupled plasma mass spectrometry. *At Spectrosc* 2011;32:175–81.
- [106] Zou X, Huang YM. Solid-phase extraction based on polyethyleneimine-modified eggshell membrane coupled with FAAS for the selective determination of trace copper(II) ions in environmental and food samples. *Anal Methods* 2013;5:6486–93.
- [107] Zhang YJ, Wang WD, Li L, Huang YM, Cao J. Eggshell membrane-based solid-phase extraction combined with hydride generation atomic fluorescence spectrometry for trace arsenic(V) in environmental water samples. *Talanta* 2010;80:1907–12.
- [108] Yang T, Chen ML, Hu XW, Wang ZW, Wang JH, Dasgupta PK. Thiolated eggshell membranes sorb and speciate inorganic selenium. *Analyst* 2011;136:83–9.
- [109] Cheng XZ, Liu J, Zou SF, Cheng K. Monitoring of heavy metal cadmium in environmental water sample by eggshell membrane preconcentration coupled with GF-AAS. 2011 International Conference on Electric Technology and Civil Engineering (ICETCE 2011) - Proceedings. 2011. p. 1356–1359.
- [110] Chen H, Liu J, Cheng X, Peng Y. Adsorption for the removal of malachite green by using eggshell membrane in environment water samples. *Adv Mater Res* 2012;573–754:63–7.
- [111] Ning L, Tao L. Adsorption and decoloration of nitroso dye based on eggshell membrane. *Adv Mater Res* 2011;183–185:963–6.
- [112] Liu J, Cheng XZ, Qin P, Pan MY. Remove of congo red from wastewater by adsorption onto eggshell membrane. *Adv Mater Res* 2012;599:391–4.
- [113] Liu T. Treatment of model wastewater including Eriochrome Black T based on eggshell membrane. *Adv Mater Res* 2011;183–185:2120–3.
- [114] Wang WD, Chen B, Huang YM, Cao J. Evaluation of eggshell membrane-based bio-adsorbent for solid-phase extraction of linear alkylbenzene sulfonates coupled with high-performance liquid chromatography. *J Chromatogr A* 2010;1217:5659–64.
- [115] Zhang Y, Jia WJ, Cui M, Dong CA, Shuang SM, Leung YK, et al. Glucose biosensor based on nanohybrid material of gold nanoparticles and glucose oxidase on a bioplatform. *Biotechnol J* 2011;6:492–500.
- [116] Wang F, Yao J, Si Y, Chen HL, Russel M, Chen K, et al. Short-time effect of heavy metals upon microbial community activity. *J Hazard Mater* 2010;173:510–6.
- [117] Liu W, Wu H, Li B, Dong C, Choi MMF, Shuang S. Immobilization of platinum nanoparticles and glucose oxidase on eggshell membrane for glucose detection. *Anal Methods* 2013;5:5154–60.
- [118] Li BX, Lan D, Zhang ZJ. Chemiluminescence flow-through biosensor for glucose with eggshell membrane as enzyme immobilization platform. *Anal Biochem* 2008;374:64–70.
- [119] Chen WW, Li BX, Xu CL, Wang L. Chemiluminescence flow biosensor for hydrogen peroxide using DNAzyme immobilized on eggshell membrane as a thermally stable biocatalyst. *Biosens Bioelectron* 2009;24:2534–40.
- [120] Song NN, Jiang HX, Cui TL, Chang LL, Wang XJ. Synthesis and enhanced gas-sensing properties of mesoporous hierarchical alpha-Fe₂O₃ architectures from an eggshell membrane. *Micro Nano Lett* 2012;7:943–6.
- [121] Joshi P, Joshi HC, Sanghi SK, Kundu S. Immobilization of monoamine oxidase on eggshell membrane and its application in designing an amperometric biosensor for dopamine. *Microchim Acta* 2010;169:383–8.
- [122] Tembe S, Kubal BS, Karve M, D'Souza SF. Glutaraldehyde activated eggshell membrane for immobilization of tyrosinase from *Amorphophallus* companulatus: application in construction of electrochemical biosensor for dopamine. *Anal Chim Acta* 2008;612:212–7.
- [123] Yeni F, Odaci D, Timur S. Use of eggshell membrane as an immobilization platform in microbial sensing. *Anal Lett* 2008;41:2743–58.
- [124] Wen G, Li Z, Choi MMF. Detection of ethanol in food: A new biosensor based on bacteria. *J Food Eng* 2013;118:56–61.
- [125] D'Souza SF, Kumar J, Jha SK, Kubal BS. Immobilization of the urease on eggshell membrane and its application in biosensor. *Mater Sci Eng C* 2013;33:850–4.
- [126] Maeda K, Sasaki Y. An experience of hen-egg membrane as a biological dressing. *Burns* 1984;8:313–6.
- [127] Mogosanu GD, Grumezescu AM. Natural and synthetic polymers for wounds and burns dressing. *Int J Pharm* 2014;463:127–36.
- [128] Ruff KJ, DeVore DP, Leu MD, Robinson MA. Eggshell membrane: a possible new natural therapeutic for joint and connective tissue disorders. Results from two open-label human clinical studies. *Clin Interv Aging* 2009;4:235–40.
- [129] Ruff KJ, Winkler A, Jackson RW, DeVore DP, Ritz BW. Eggshell membrane in the treatment of pain and stiffness from osteoarthritis of the knee: a randomized, multicenter, double-blind, placebo-controlled clinical study. *Clin Rheumatol* 2009;28:907–14.
- [130] Benson KF, Ruff KJ, Jensen GS. Effects of natural eggshell membrane (NEM) on cytokine production in cultures of peripheral blood mononuclear cells: increased suppression of tumor necrosis factor-alpha levels after in vitro digestion. *J Med Food* 2012;15:360–8.
- [131] Hirata A, Iwakiri R, Okinami S. A simulated eye for vitreous surgery using Japanese quail eggs. *Graefes Arch Clin Exp Ophthalmol* 2013;251:1621–4.
- [132] Farjah GH, Heshmatian B, Karimpour M, Saberi A. Using eggshell membrane as nerve guide channels in peripheral nerve regeneration. *Iran J Bas Med Sci* 2013;16:901–5.
- [133] Tao YY, Lu YF, Sun YJ, Gu B, Lu WY, Pan J. Development of mucoadhesive microspheres of acyclovir with enhanced bioavailability. *Int J Pharm* 2009;378:30–6.
- [134] Poland AL, Sheldon BW. Altering the thermal resistance of foodborne bacterial pathogens with an eggshell membrane waste by-product. *J Food Prot* 2001;64:486–92.
- [135] Mine Y, Oberle C, Kassify Z. Eggshell matrix proteins as defense mechanism of avian eggs. *J Agric Food Chem* 2003;51:249–53.

- [136] Deng WT, Liu Y, Zhang Y, Lu F, Chen QY, Ji XB. Enhanced electrochemical capacitance of nanoporous NiO based on an eggshell membrane. *RSC Adv* 2012;2:1743–5.
- [137] Li Z, Zhang L, Amirkhiz BS, Tan XH, Xu ZW, Wang HL, et al. Carbonized chicken eggshell membranes with 3D architectures as high-performance electrode materials for supercapacitors. *Adv Energy Mater* 2012;2:431–7.
- [138] Chung SH, Manthiram A. Carbonized eggshell membrane as a natural polysulfide reservoir for highly reversible Li-S batteries. *Adv Mater* 2013. in press, <http://dx.doi.org/10.1002/adma.201304365>.
- [139] Yu HJ, Tang QQ, Wu JH, Lin YZ, Fan LQ, Huang ML, et al. Using eggshell membrane as a separator in supercapacitor. *J Power Sources* 2012; 206:463–8.
- [140] Neelakandeswari N, Sangami G, Dharmaraj N. Preparation and characterization of nanostructured hydroxyapatite using a biomaterial. *Synth React Inorg Met-Org Nano-Met Chem* 2011;41:513–6.
- [141] Wang Q, Liu X, Zhang LC, Lv Y. Microwave-assisted synthesis of carbon nanodots through an eggshell membrane and their fluorescent application. *Analyst* 2012;137:5392–7.
- [142] Baláž M, Baláž P, Sayagués MJ, Zorkovská A. Bio-inspired mechanochemical synthesis of semiconductor nanomaterial using eggshell membrane. *Mater Sci Semicond Process* 2013;16:1899–903.
- [143] Baláž P, Achimovičová M, Baláž M, Billik P, Cherkezova-Zheleva Z, Criado JM, et al. Hallmarks of mechanochemistry: from nanoparticles to technology. *Chem Soc Rev* 2013;42:7571–637.
- [144] Baláž P. Mechanochemistry in Nanoscience and Minerals Engineering. Berlin: Springer Verlag; 2008.
- [145] Chai Z, Li YY, Liu F, Du BJ, Jiao T, Zhang CY, et al. Outer eggshell membrane as delivery vehicle for polysaccharide/protein microcapsules incorporated with vitamin E. *J Agric Food Chem* 2013;61:589–95.
- [146] Trimbos KB, Broekman J, Kentie R, Musters CJM, de Snoo GR. Using eggshell membranes as a DNA source for population genetic research. *J Ornithol* 2009;150:915–20.
- [147] Yi F, Yu J, Li Q, Guo ZX. Soluble eggshell membrane protein: antibacterial property and biodegradability. *J Wuhan Univ Technol* 2007;22:117–9.
- [148] Kang J, Kotaki M, Okubayashi S, Sukigara S. Fabrication of electrospun eggshell membrane nanofibers by treatment with catechin. *J Appl Polym Sci* 2010;117:2042–9.
- [149] Kim GH, Min T, Park SA, Kim WD. Coaxially electrospun micro/nanofibrous poly(epsilon-caprolactone)/eggshell-protein scaffold. *Bioinsp Biomim* 2008;3:016006.
- [150] Jia J, Liu G, Guo ZX, Yu J, Duan YY. Preparation and characterization of soluble eggshell membrane protein/PLGA electrospun nanofibers for guided tissue regeneration membrane. *J Nanomater* 2012;282736.
- [151] Lu JW, Li Q, Qi QL, Guo ZX, Yu J. Surface engineering of poly(D,L-lactic acid) by entrapment of soluble eggshell membrane protein. *J Biomed Mater Res A* 2009;91A:701–7.
- [152] Qi QL, Li Q, Lu JW, Guo ZX, Yu J. Preparation and characterization of soluble eggshell membrane protein/chitosan blend films. *Chin J Polym Sci* 2009;27:387–92.
- [153] Xiong X, Li Q, Lu JW, Guo ZX, Sun ZH, Yu J. Fibrous scaffolds made by co-electrospinning soluble eggshell membrane protein with biodegradable synthetic polymers. *J Biomater Sci-Polym Ed* 2012;23:1217–30.
- [154] Huang X, Zhou Y, Ma M, Cai Z, Li T. Chemiluminescence evaluation of antioxidant activity and prevention of DNA damage effect of peptides isolated from soluble eggshell membrane protein hydrolysate. *J Agric Food Chem* 2010;58:12137–42.
- [155] Sah MK, Pramanik K. Soluble-eggshell-membrane-protein-modified porous silk fibroin scaffolds with enhanced cell adhesion and proliferation properties. *J Appl Polym Sci* 2014;131. <http://dx.doi.org/10.1002/app.40138>.